

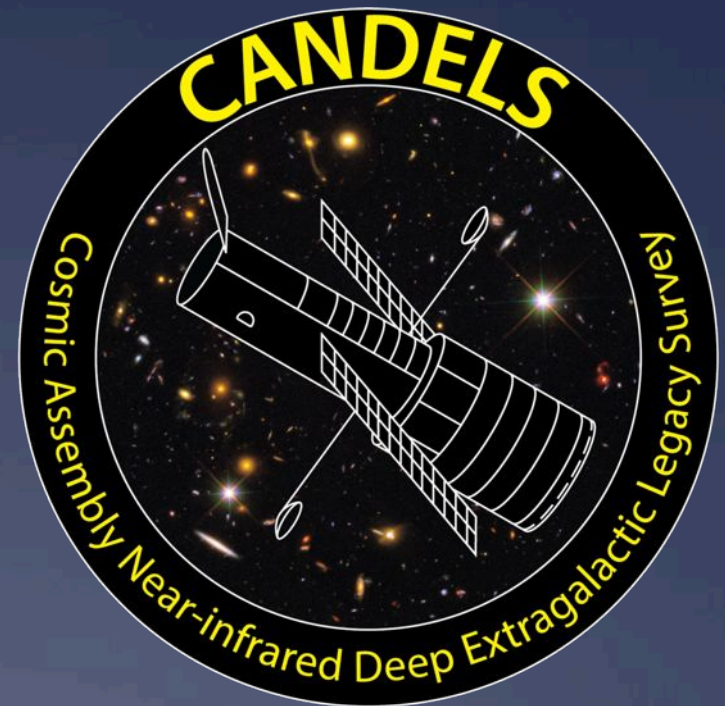
CANDELS

Greatest Hits

Sandra Faber & Henry
Ferguson

DresslerFest, Zion Park

11 September 2014



Exposure Strategy

250,000 galaxies $\sim 2 \times 10^6$ Mpc³ per unit z for $z > 1.5$

- ❖ “Wedding cake” strategy: three layers of J+H

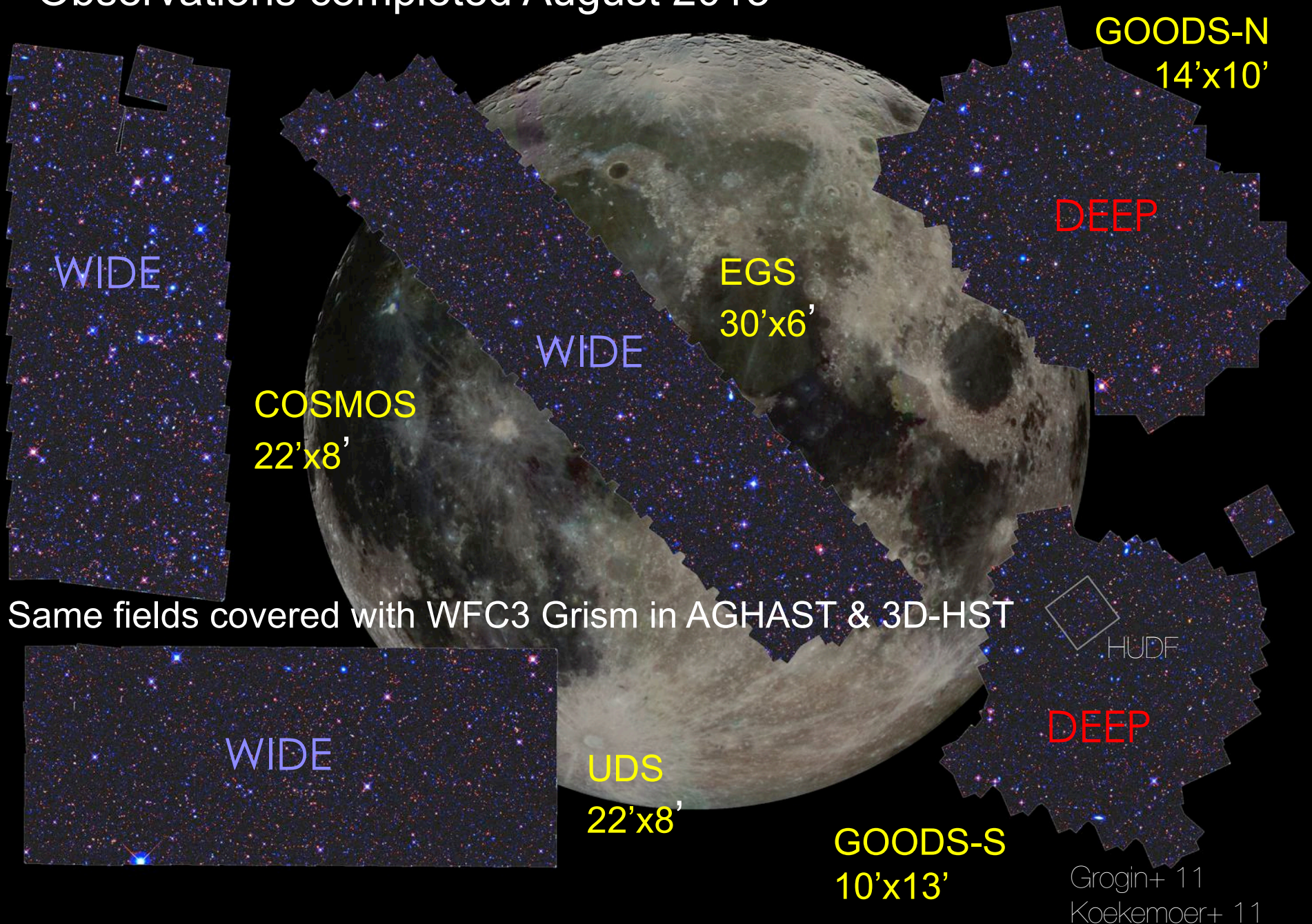
UDFs: ~ 100 orbit depth over
 ~ 10 sq arcmin

DEEP: 8 orbit depth over
 ~ 120 sq arcmin

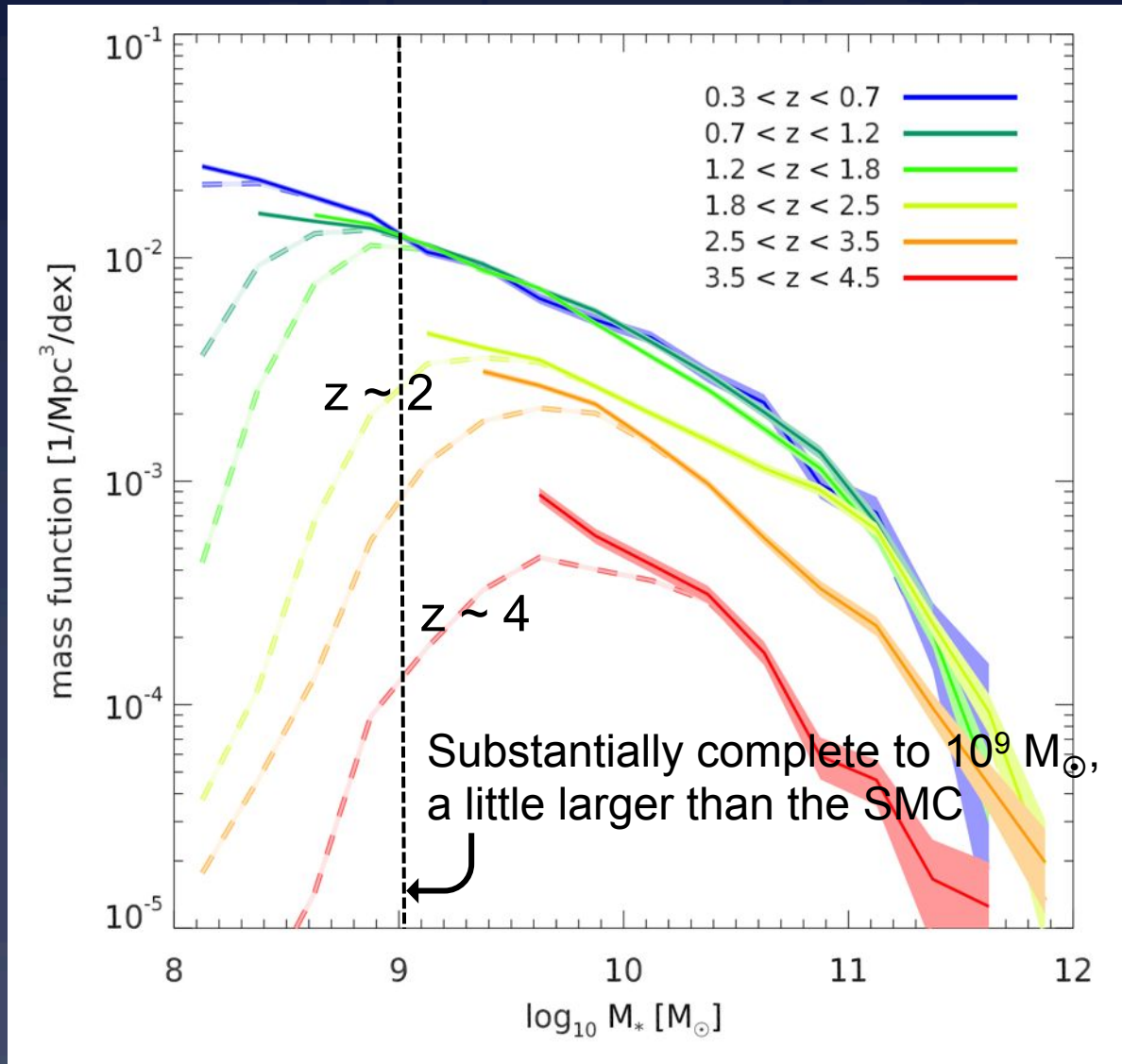
WIDE: 2 orbit depth over
 ~ 700 sq arcmin



Observations completed August 2013



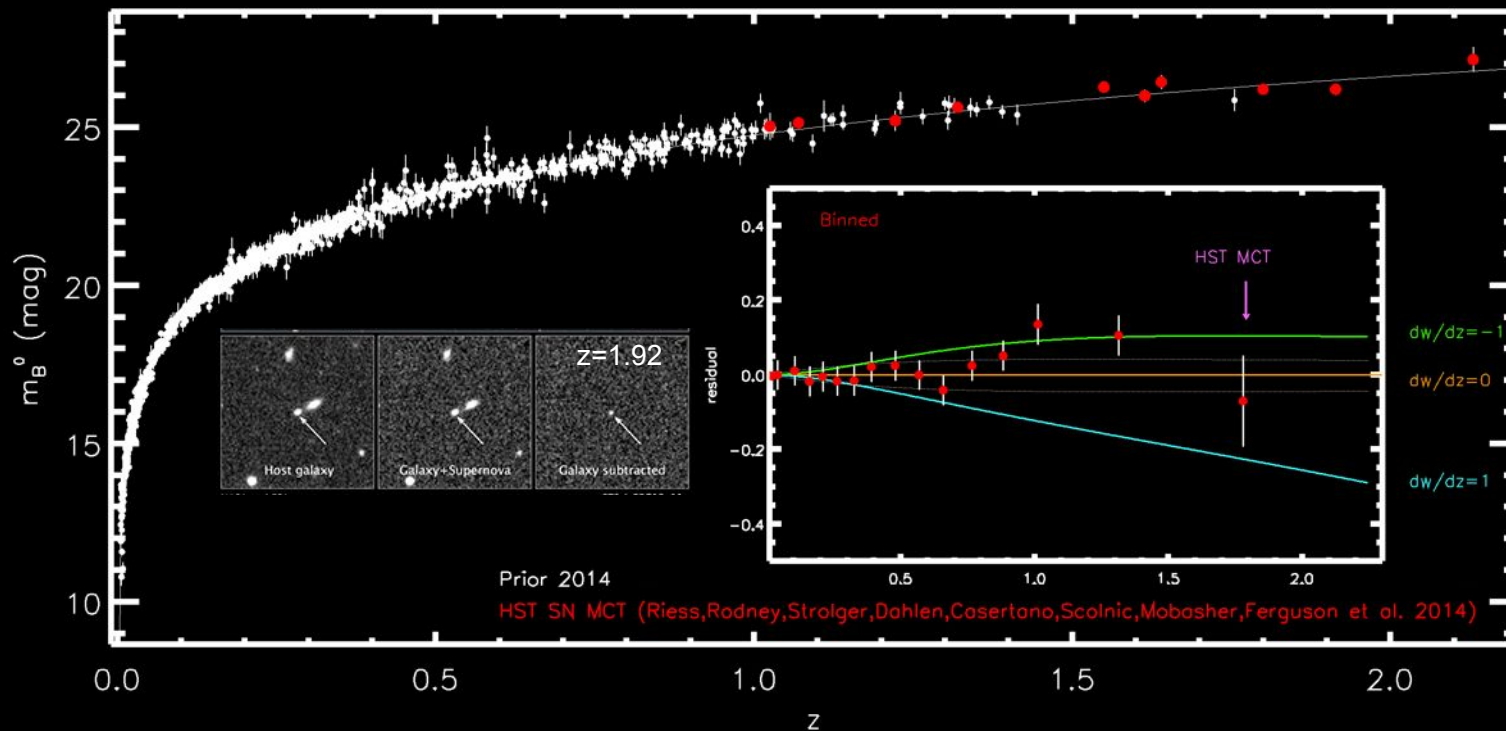
CANDELS Stellar Mass Coverage



High Redshift **1** Type 1a SNaE

Building the Modern SN Ia Hubble Diagram; **to the limit**

2014: HST SN MCT, searched CANDELS/CLASH w/ WFC3-IR, $1.5 < z < 2.1$



Established: SNe Ia to $z=2.1$, $dw/dz \sim 0 \pm 1$ still tracking model, but SN Ia at $z \sim 2$ are rare \rightarrow long progenitor fuse

High-z supernova rates

THE ASTRONOMICAL JOURNAL, 148:13 (28pp), 2014 July

RODNEY ET AL.

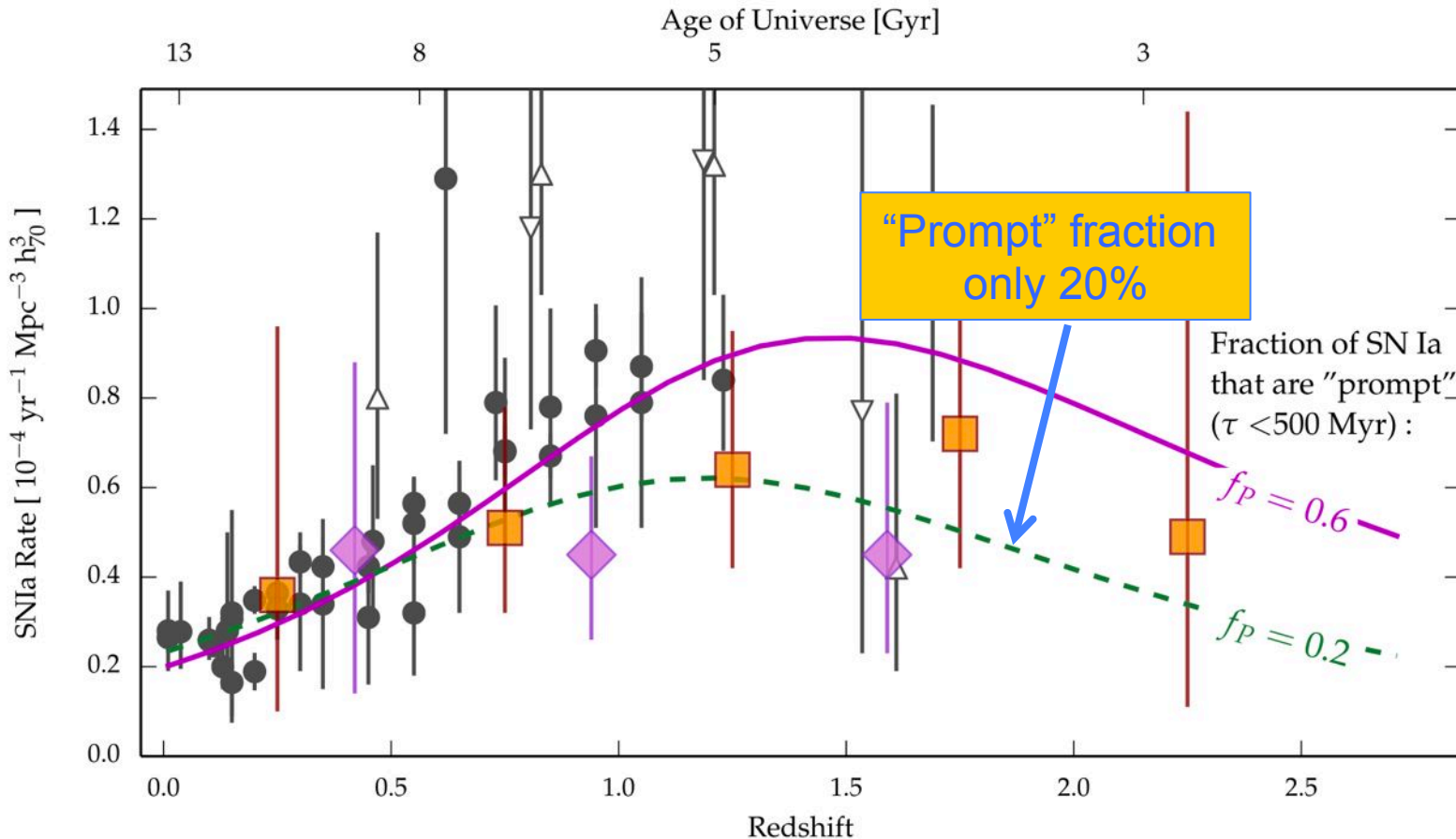
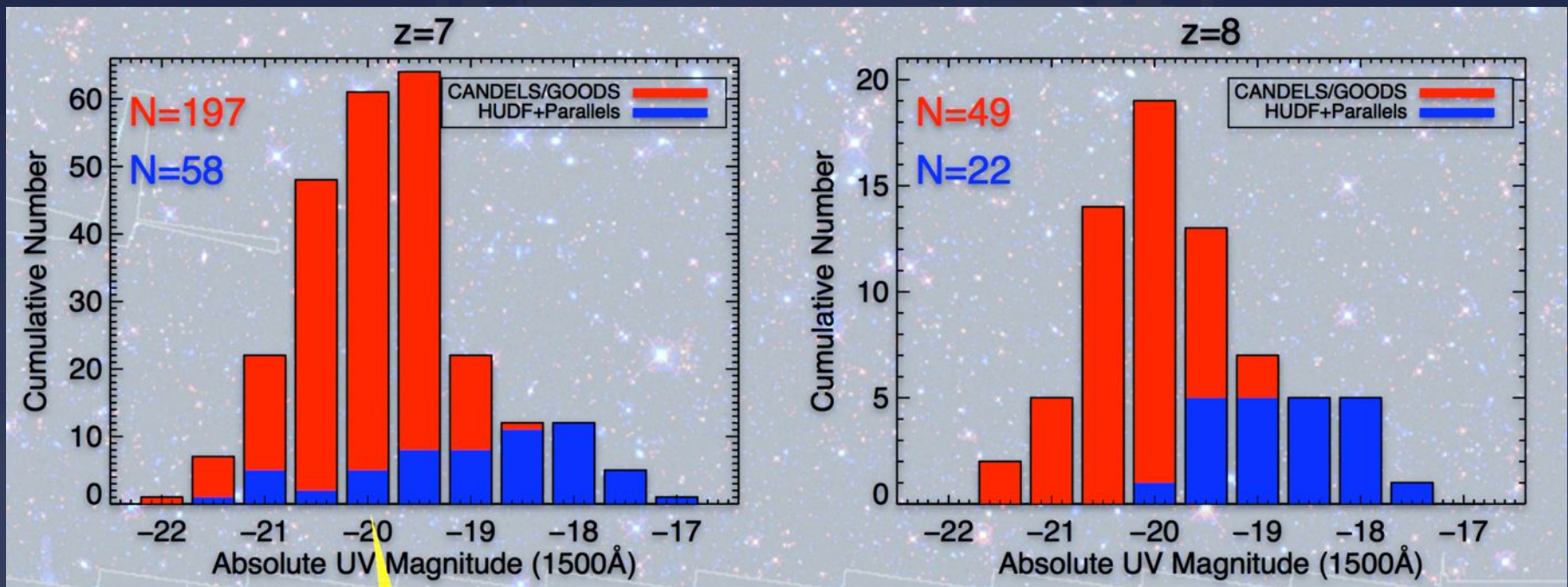


Figure 11. Comparing observed SN rates against DTD models. Gray markers show the collection of rates from the literature, using filled points for the ground-based surveys and open symbols for past *HST* surveys. As in Figure 9, large purple diamonds show the CLASH rates from Graur et al. (2014) and large orange squares show the CANDELS rates from this work. In this figure, vertical error bars show only the statistical uncertainties. Two curves show the SN Ia rates predicted by assuming a DTD that is proportional to t^{-1} for all times above 500 Myr, but with different assumptions for the fraction of SNe Ia that are prompt. The magenta solid line shows the best fit to the ground-based data (solid gray points), which has $\sim 60\%$ of all SNe Ia exploding within 500 Myr of birth. The green dashed line is the best-fit model when using the CANDELS+CLASH data alone, for which the prompt SN Ia fraction is $\sim 20\%$.

2 Cosmic Dawn Galaxies

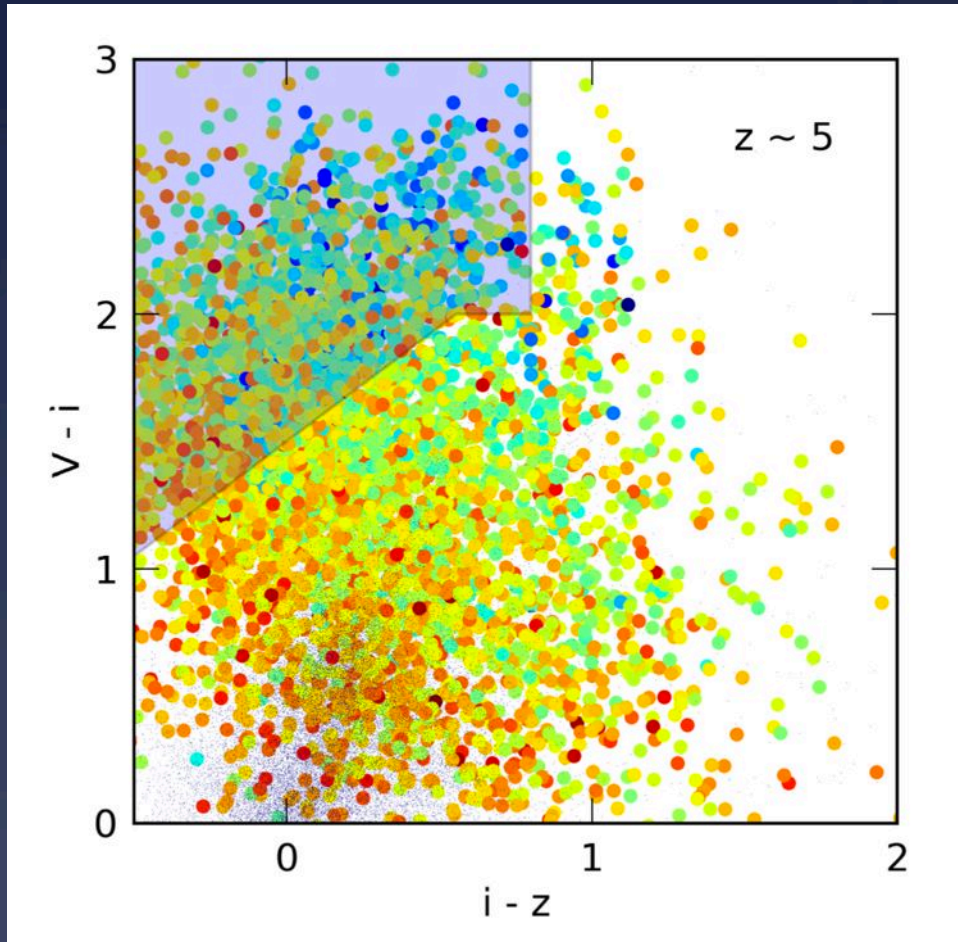
The Need for CANDELS at High z

Larger fields, more rare/bright galaxies



The Need for CANDELS at High z

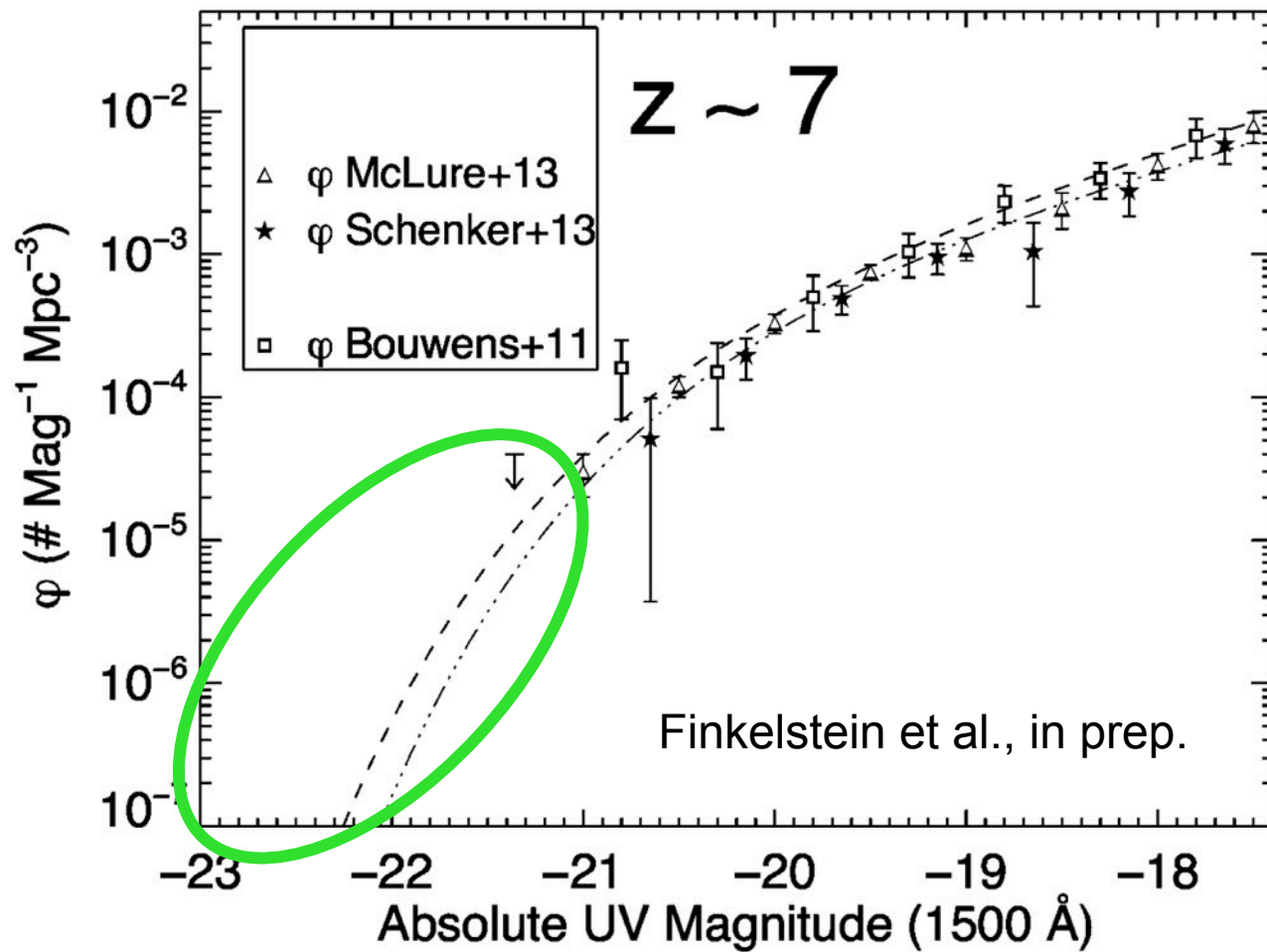
Full multi-wave SED modeling



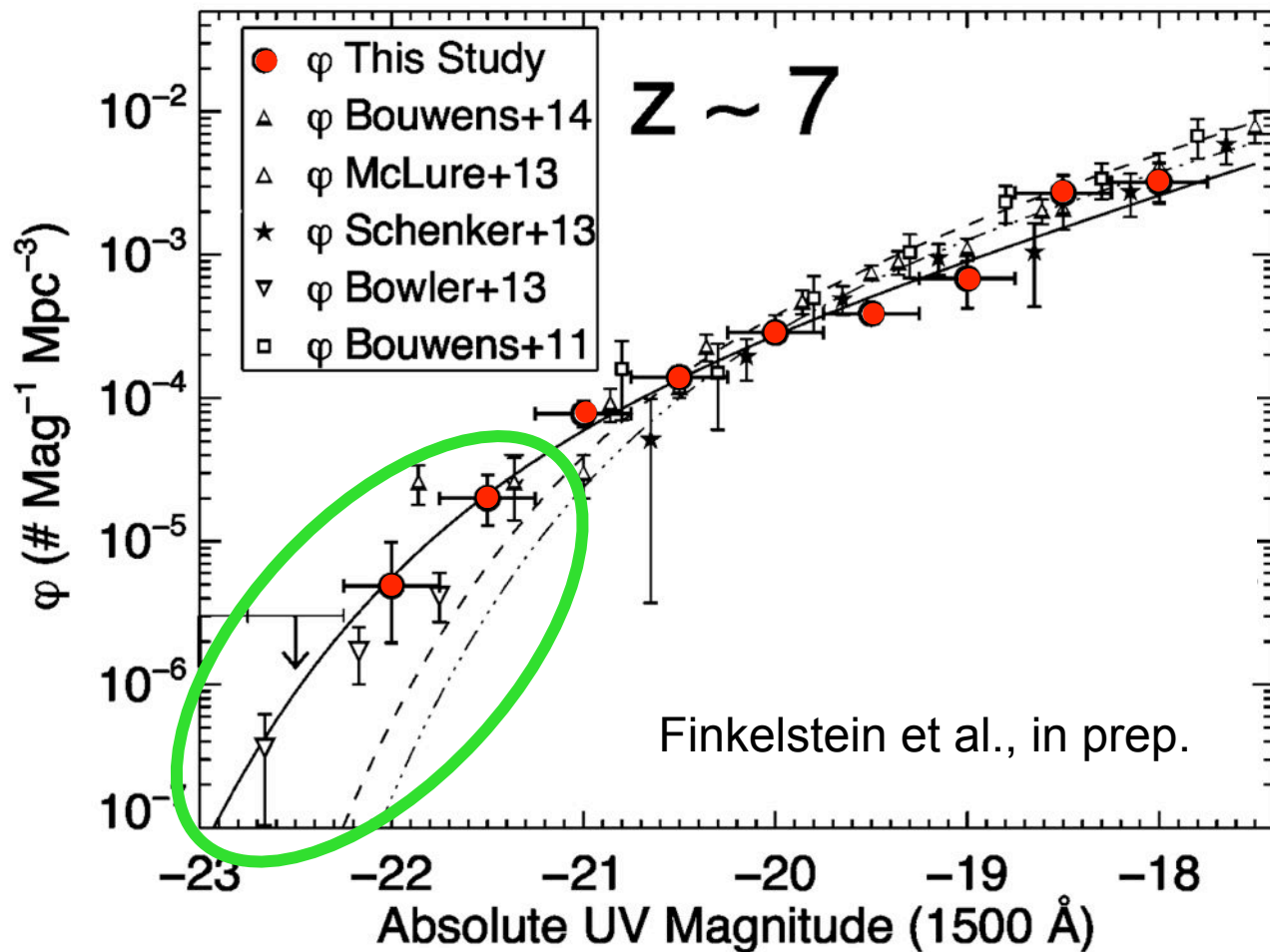
- Adding photometric scatter:
 - Many galaxies do not meet traditional Lyman-break criteria

Duncan+ 14 submitted

There are more high-z galaxies than we thought

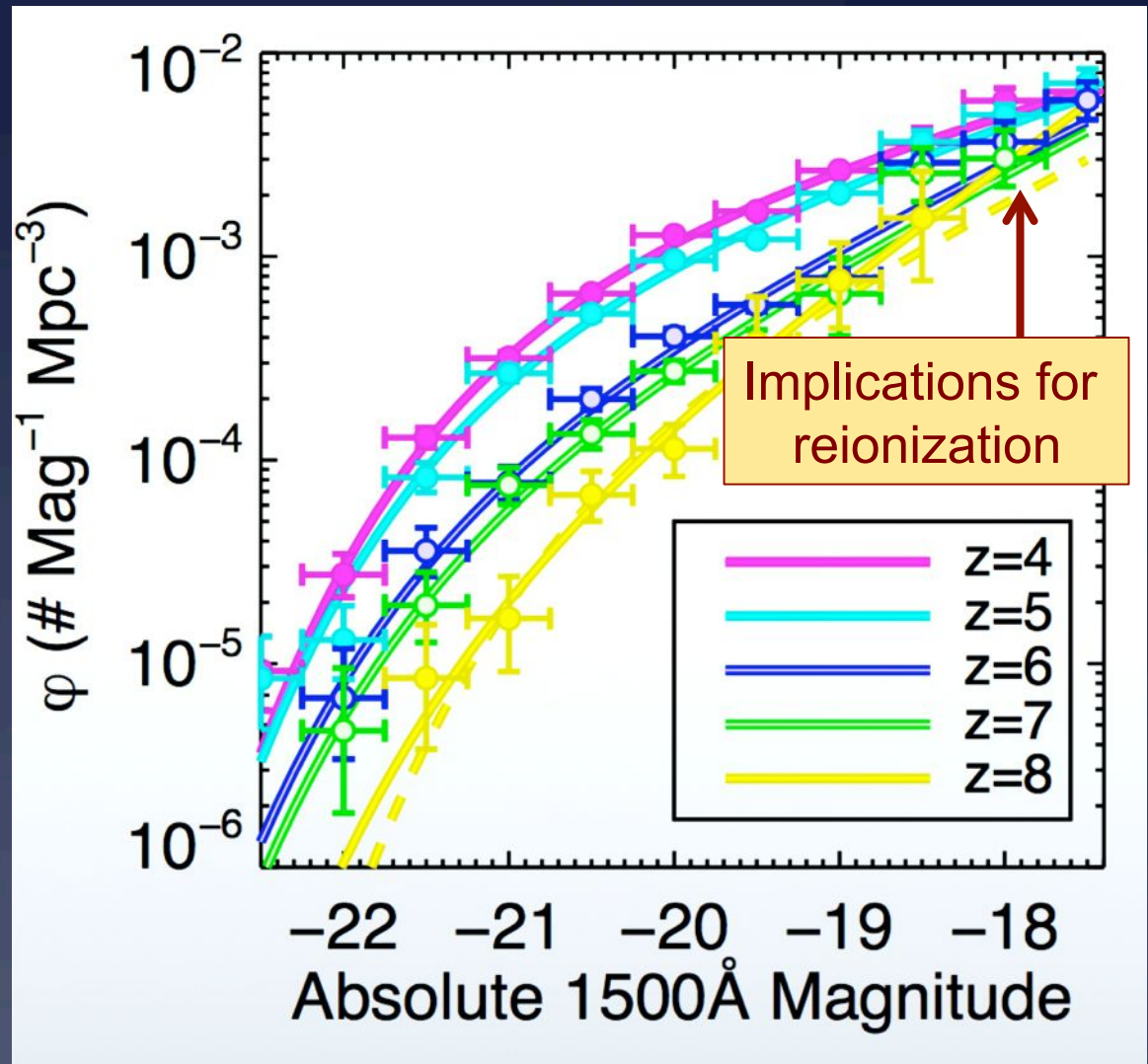


There are more high- z galaxies than we thought



The early lum. function evolves dramatically

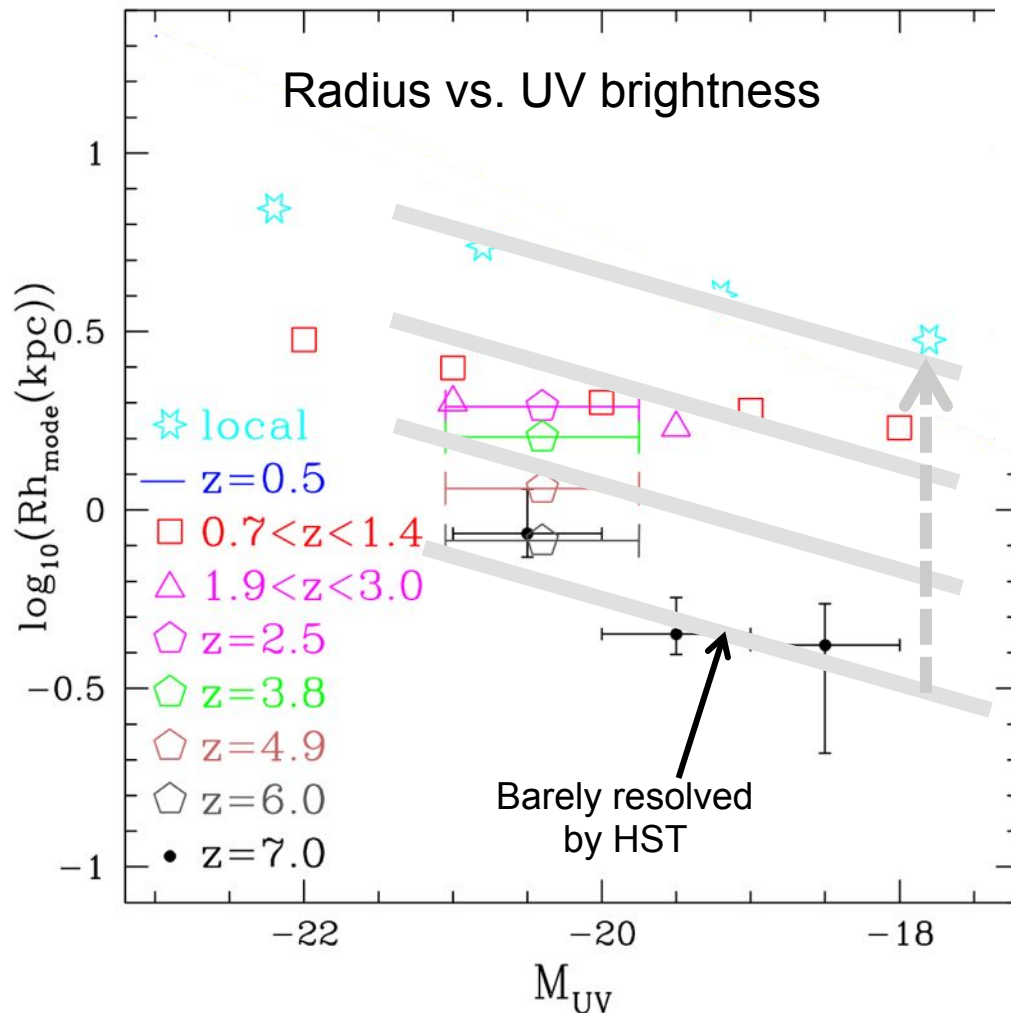
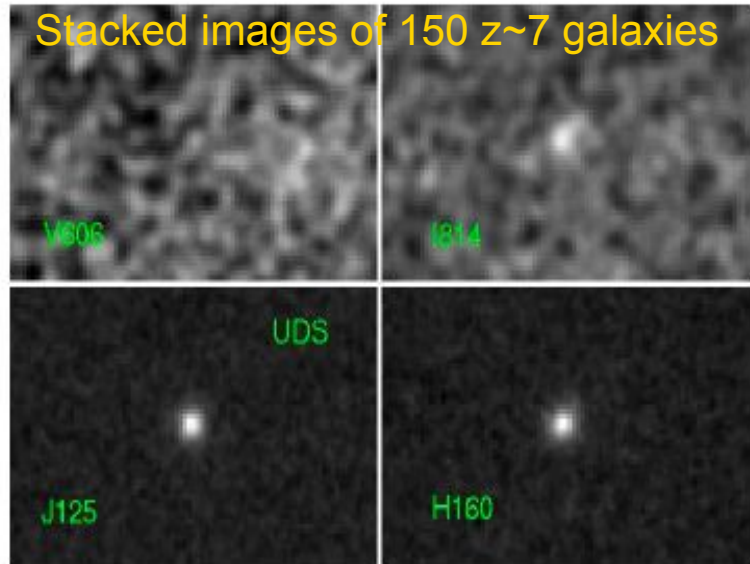
- Bright end evolves faster
- Global tilt declines with time
- Early steep slope has major implications for total SFR and UV density for reionization



Finkelstein et al., in prep.

$z \sim 7$ galaxies are barely resolved “nuggets”

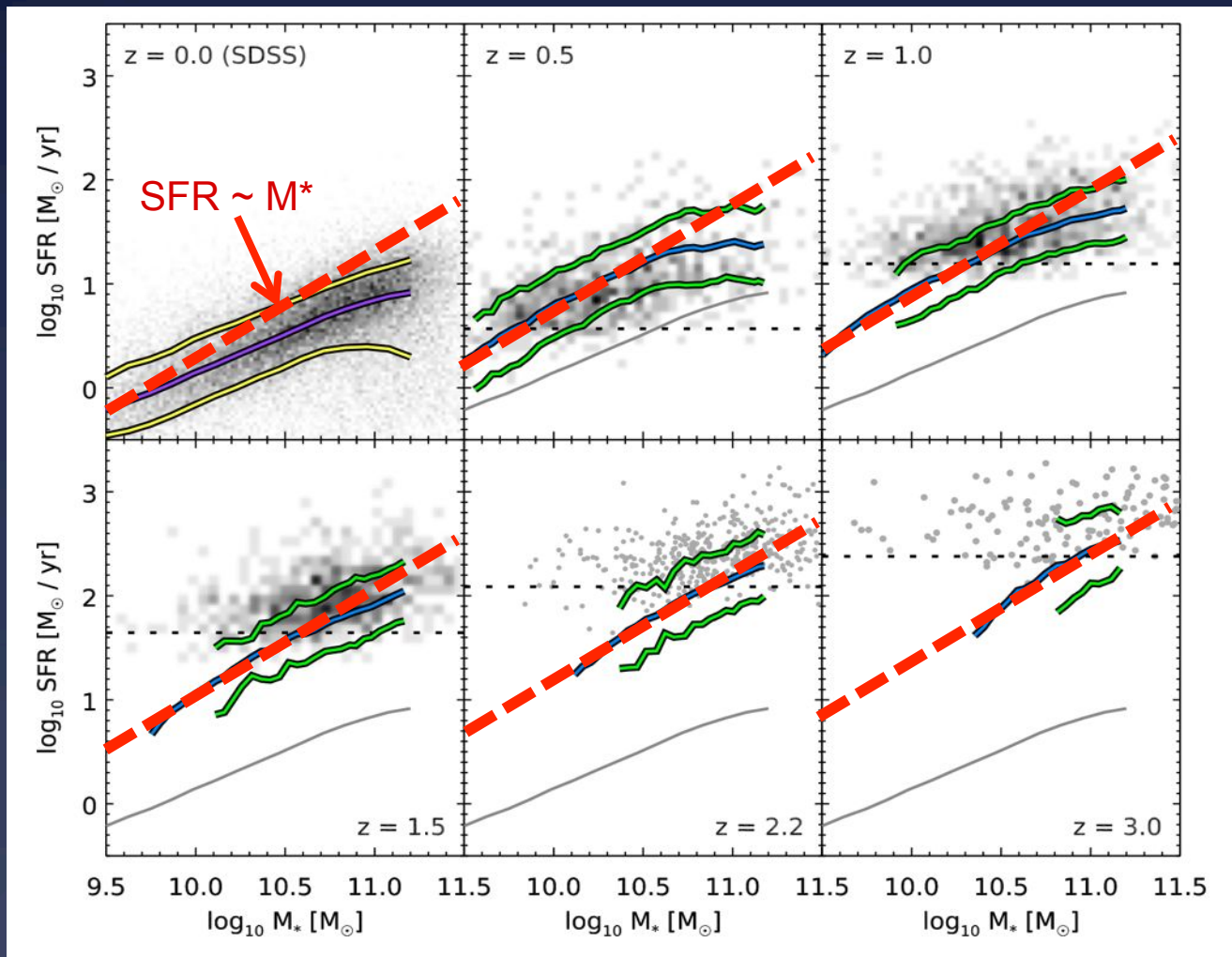
Grazian+ 12



- Resolvable only by stacking sources
- They do not seem to be embedded within larger low-brightness systems
- Challenge to models?

The Star-Forming Main Sequence

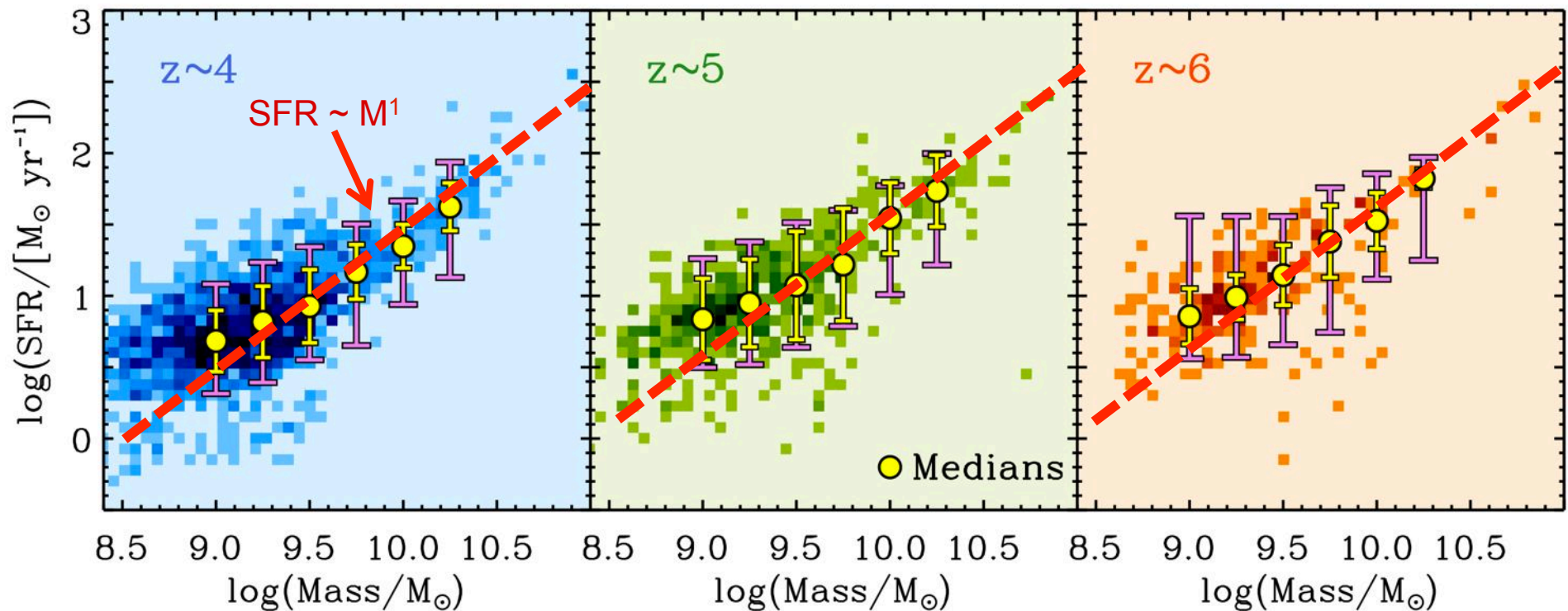
Herschel data now available to $z \sim 3$ using stacking



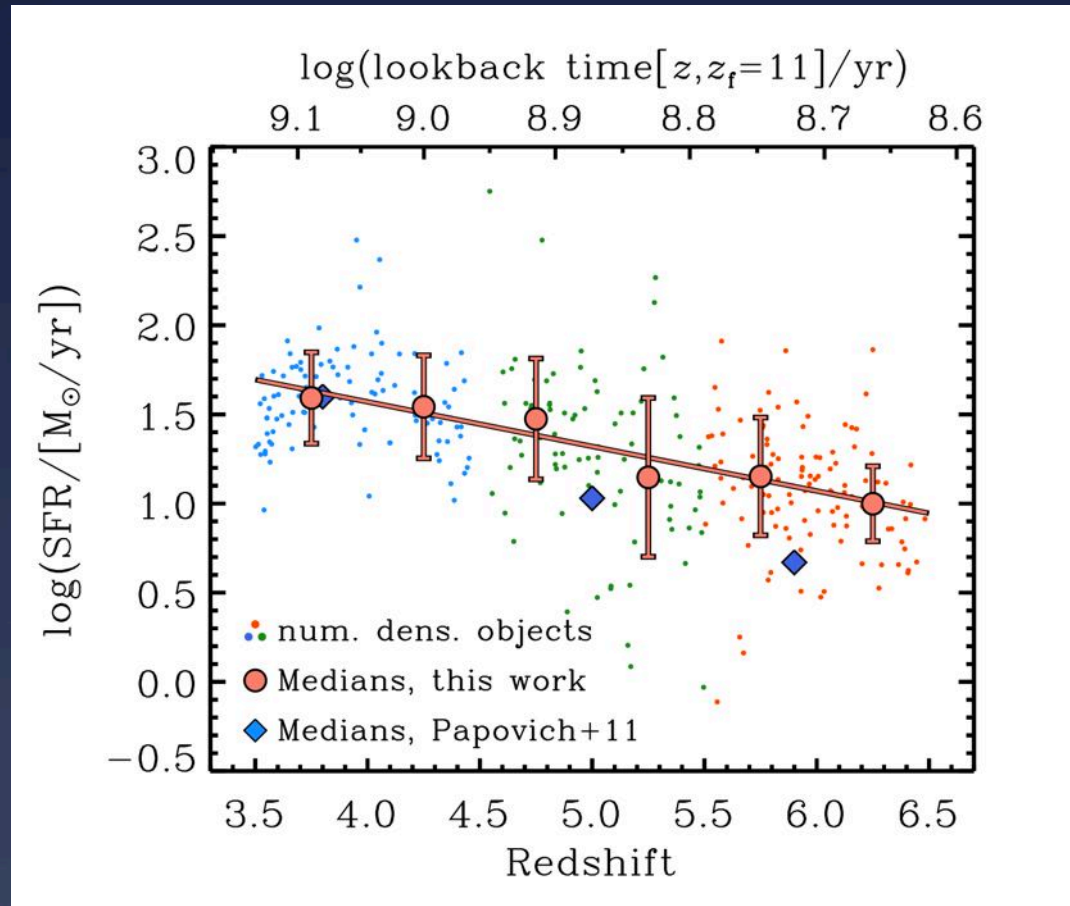
- Stacking makes Herschel go much deeper
- Slope approaches $\text{SSFR} \sim \text{const.}$ at high z

SFR “Main Sequence” continues to high z

- Narrow sequence exists to at least $z \sim 6$
- Normalization saturates beyond $z \sim 4$
- Slope approaches $\text{SFR} \sim M^*$
- Implies early rising SFR histories

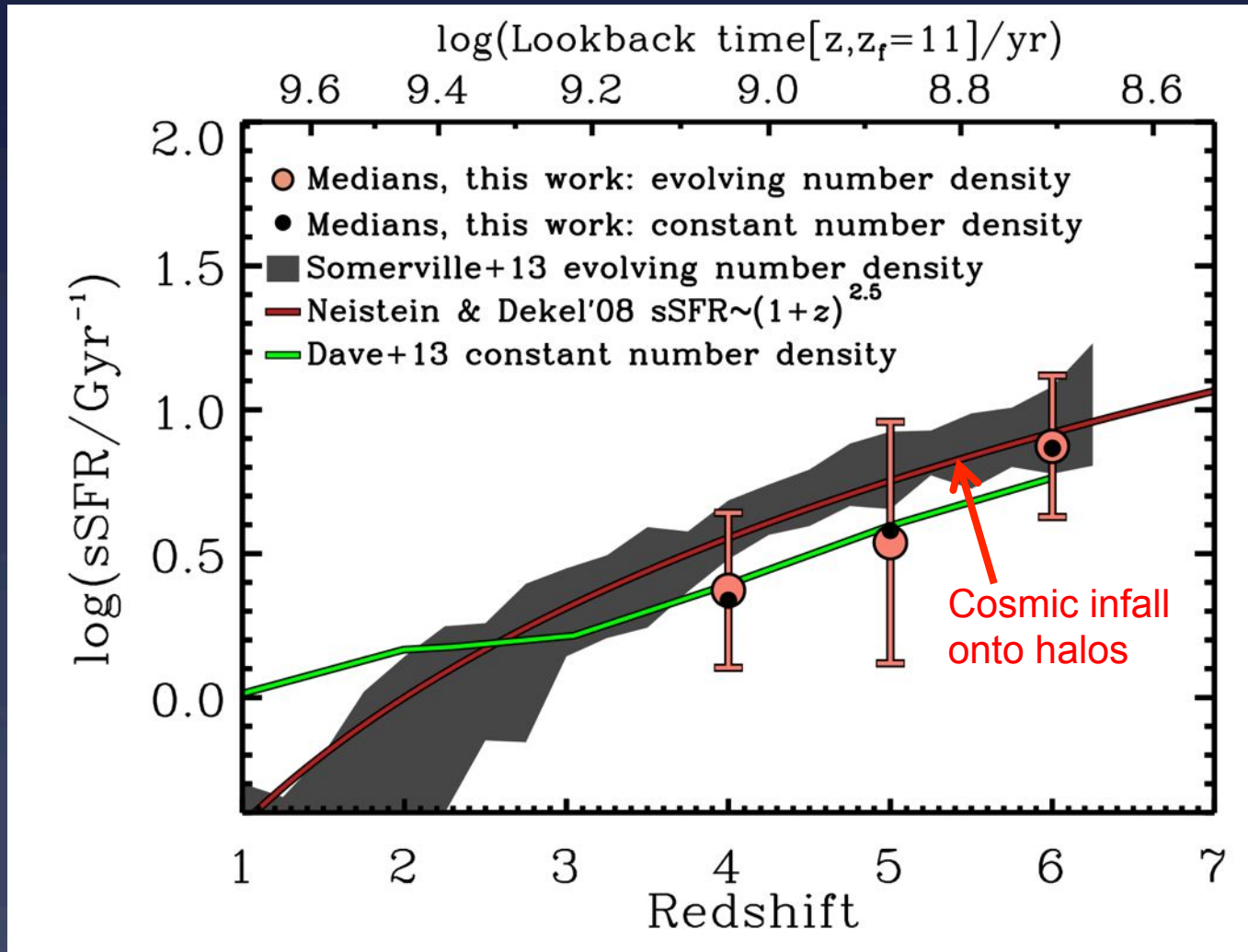


The era of rising star-formation histories has been reached

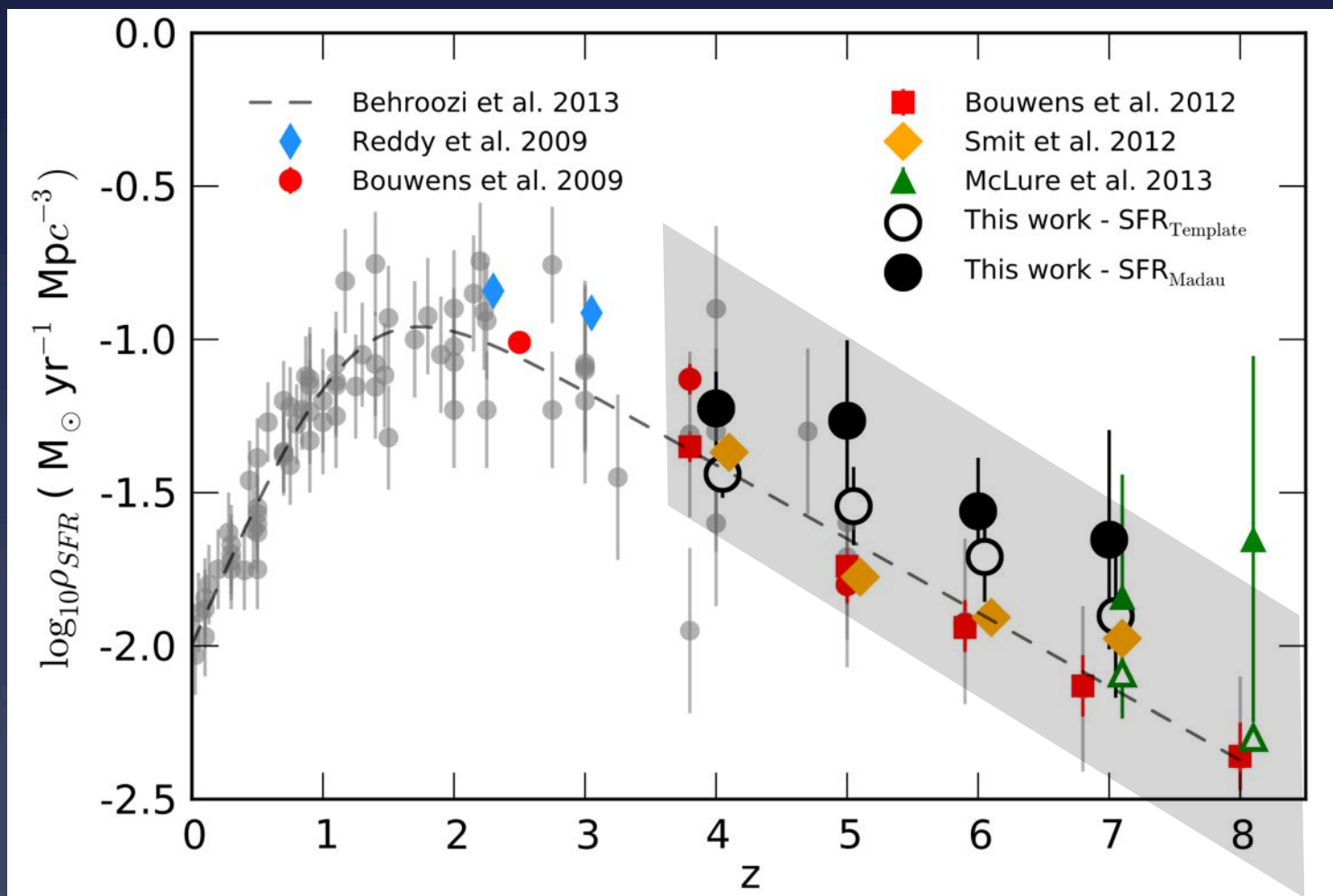


- Selecting galaxies to link mothers and daughters using dark-halo theory:
- Star-formation rates increase as $\Psi(t) \sim t^{1.4}$

SSFR of a single galaxy falls with time, as predicted



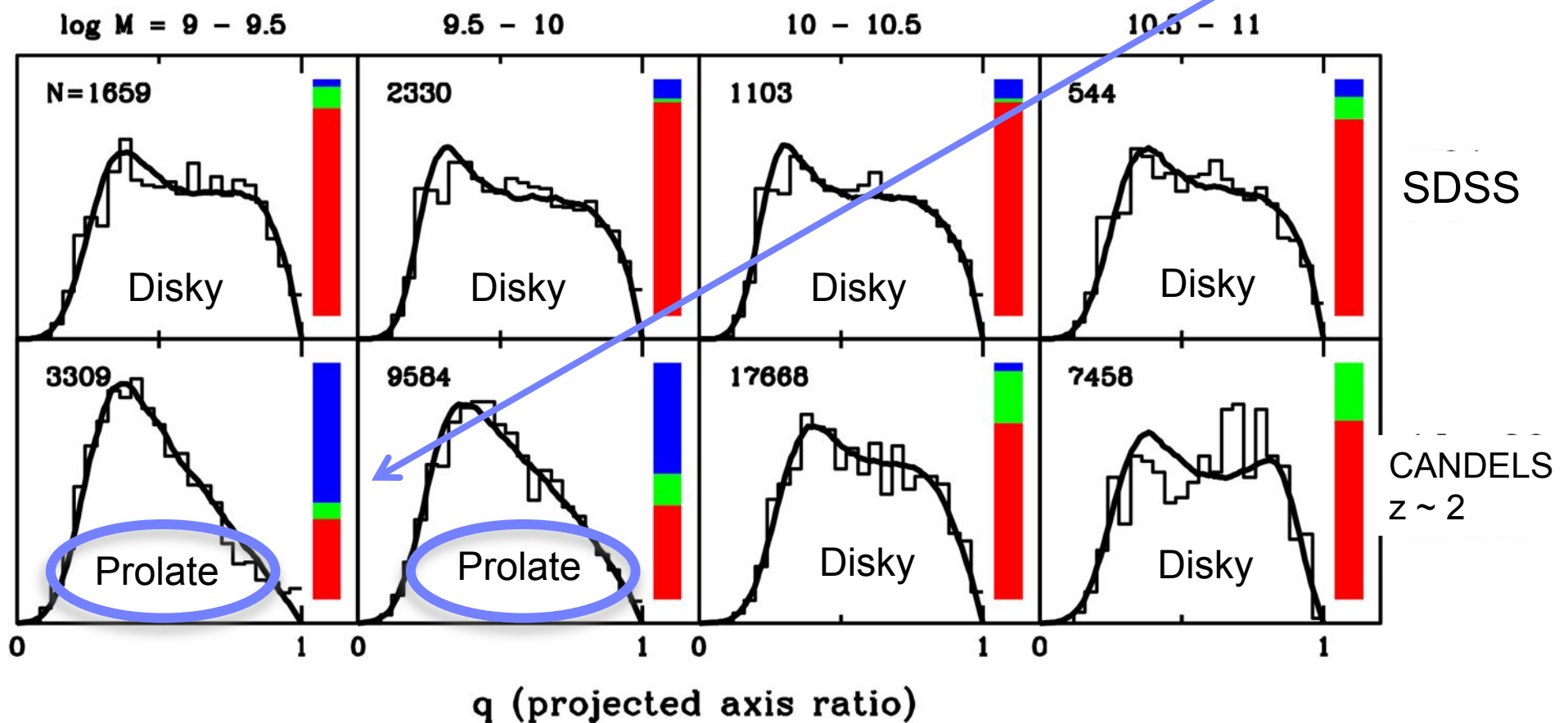
Amplitude of the early cosmic star-formation rate density is still in flux due to various unresolved corrections



Cosmic Noon Galaxies

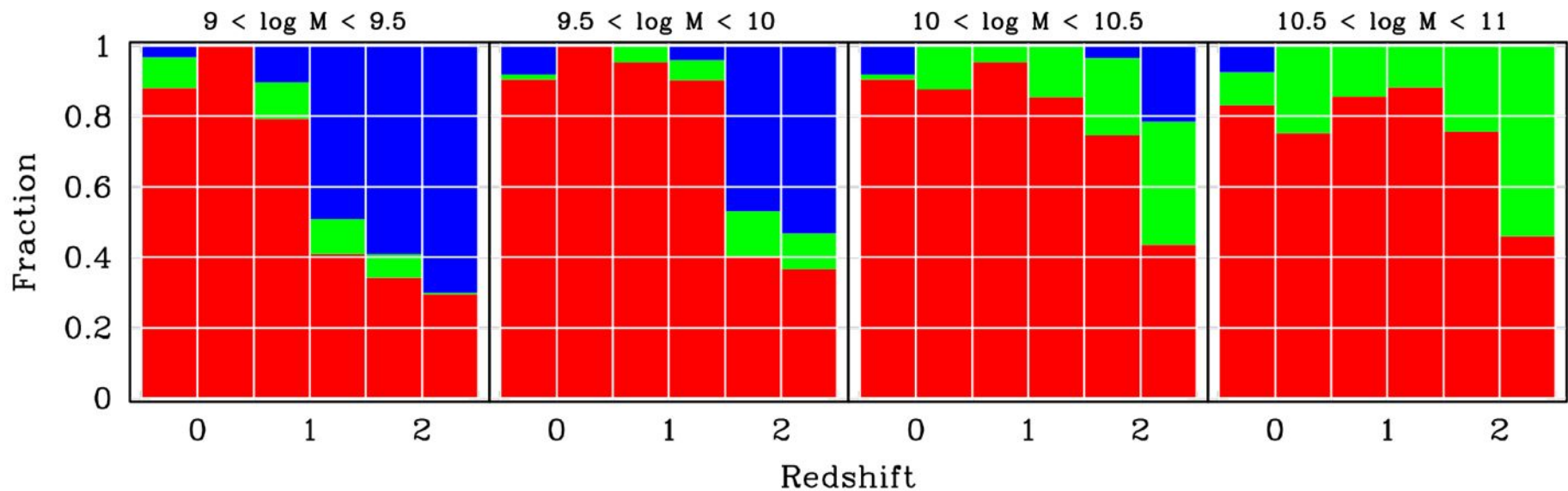
Diskiness grows with both mass and time

Axial ratio distributions of small galaxies indicate prolate



Diskiness grows with both mass and time

“Morphological downsizing”



Blue = prolate

Red = disk

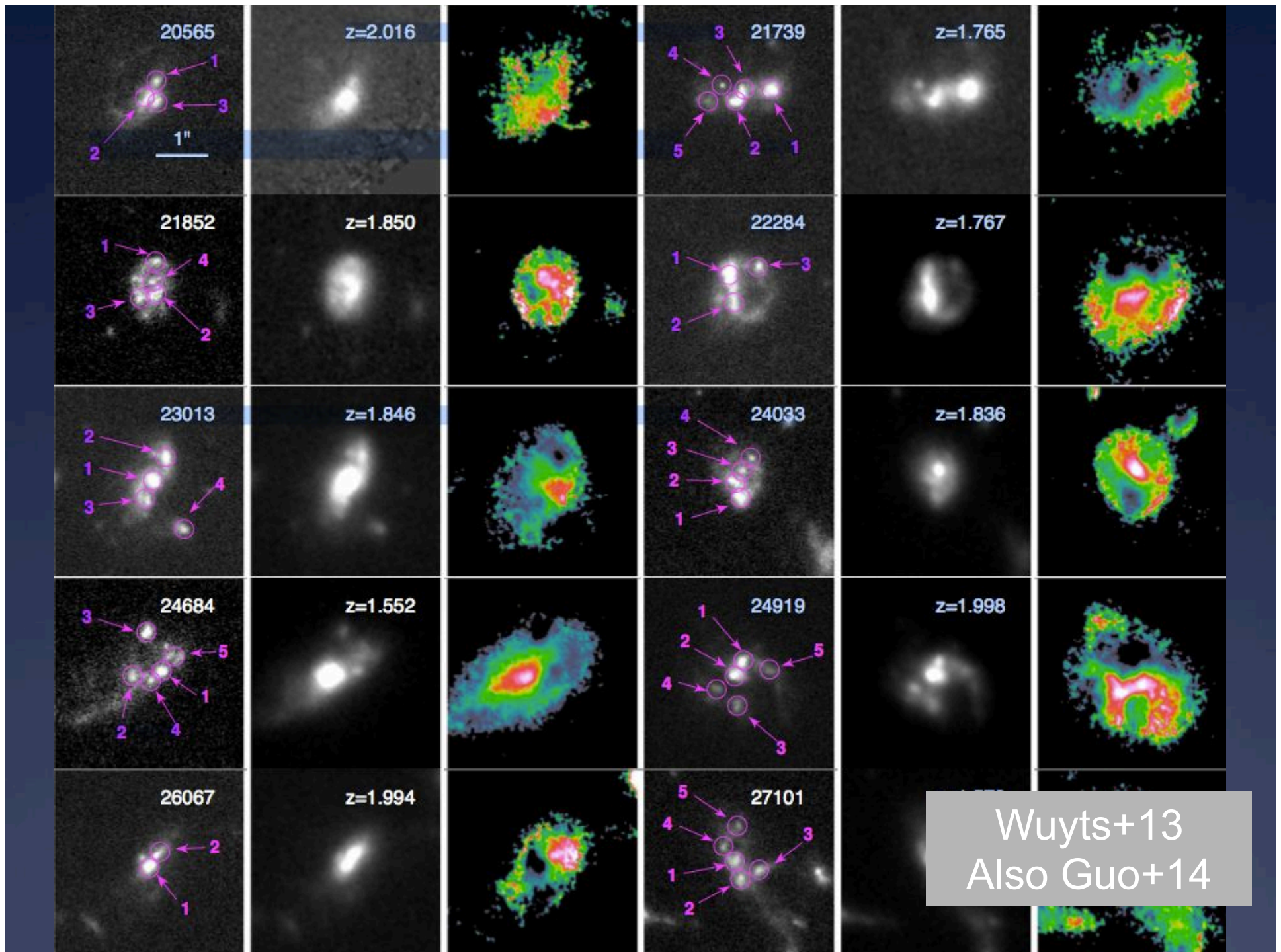
Green = spheroid

time

van der Wel+14

Prominent star-forming clumps have ages and radial trends that are consistent with models involving violent disk instabilities.

Clumps may be important for AGN fueling and galaxy bulge formation.



Statistical SED Fitting of Clumps

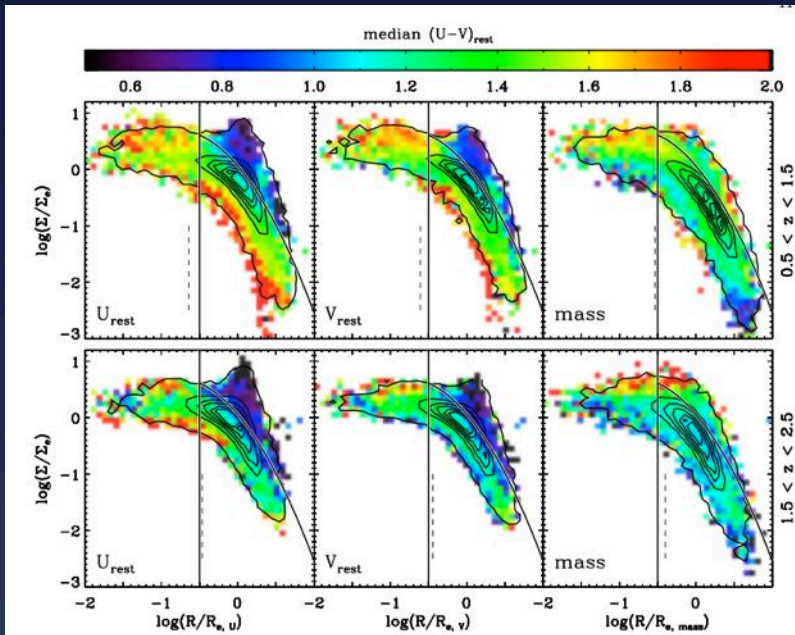


FIG. 5.— Co-added normalized profiles for the SFGs at $0.5 < z < 1.5$ (top row) and $1.5 < z < 2.5$ (bottom row), uncorrected for smearing by the PSF. F.I.T.R., the surface brightnesses/densities and half-light/mass radii were measured on the U_{rest} , V_{rest} , and stellar mass maps, always adopting the center of stellar mass as a reference for measurements of radii. The profiles are color-coded by the median rest-frame $(U - V)_{rest}$ color within each $(\Sigma_*/\Sigma_*, R/R_*)$ bin. The vertical dashed line indicates the typical resolution, and solid lines separate the center, disk and clump regime as in Figure 4. Bright, off-center clumps notable at short wavelengths, and to a lesser extent present even at the longest wavelengths attainable at high resolution, tend to be bluer than the underlying galaxy disk. The reddest colors are found in the center.

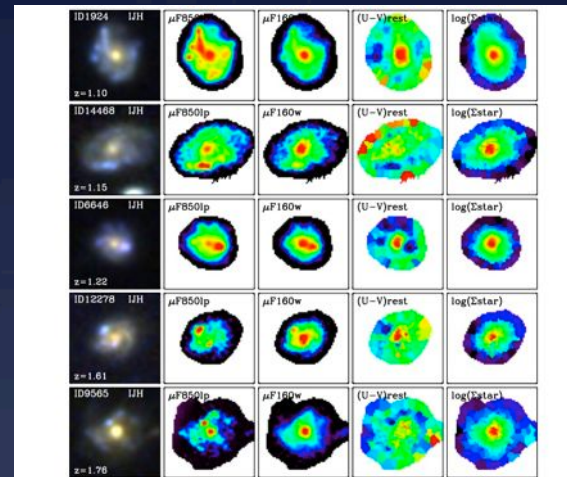


FIG. 2.— Case examples of galaxies at $z \approx 1 - 2$ exhibiting off-center peaks in the surface brightness distribution. From left to right (I.L.R.): observed I_{110}, H_{160} 3-color postage stamps and $3 \times 3 \times 3$ surface brightness distributions in the observed H_{160} and I_{110} bands, rest-frame $U - V$ color maps, and the distribution of stellar surface mass density. The off-center regions with elevated surface brightness tend to be blue, and therefore less pronounced (but still present) in H_{160} compared to I_{110} . With a few notable exceptions (ID1663 and ID1228), the stellar mass maps are centrally concentrated, and lack regions with elevated surface mass density at large radii.

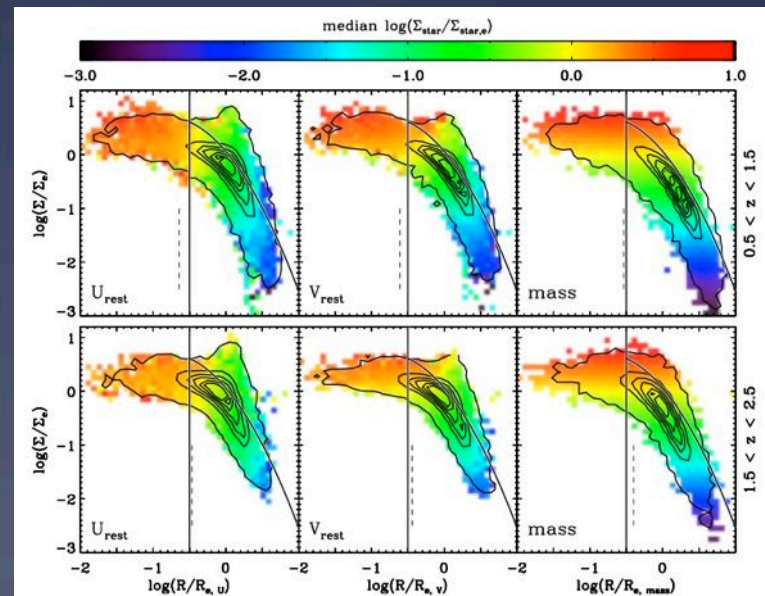


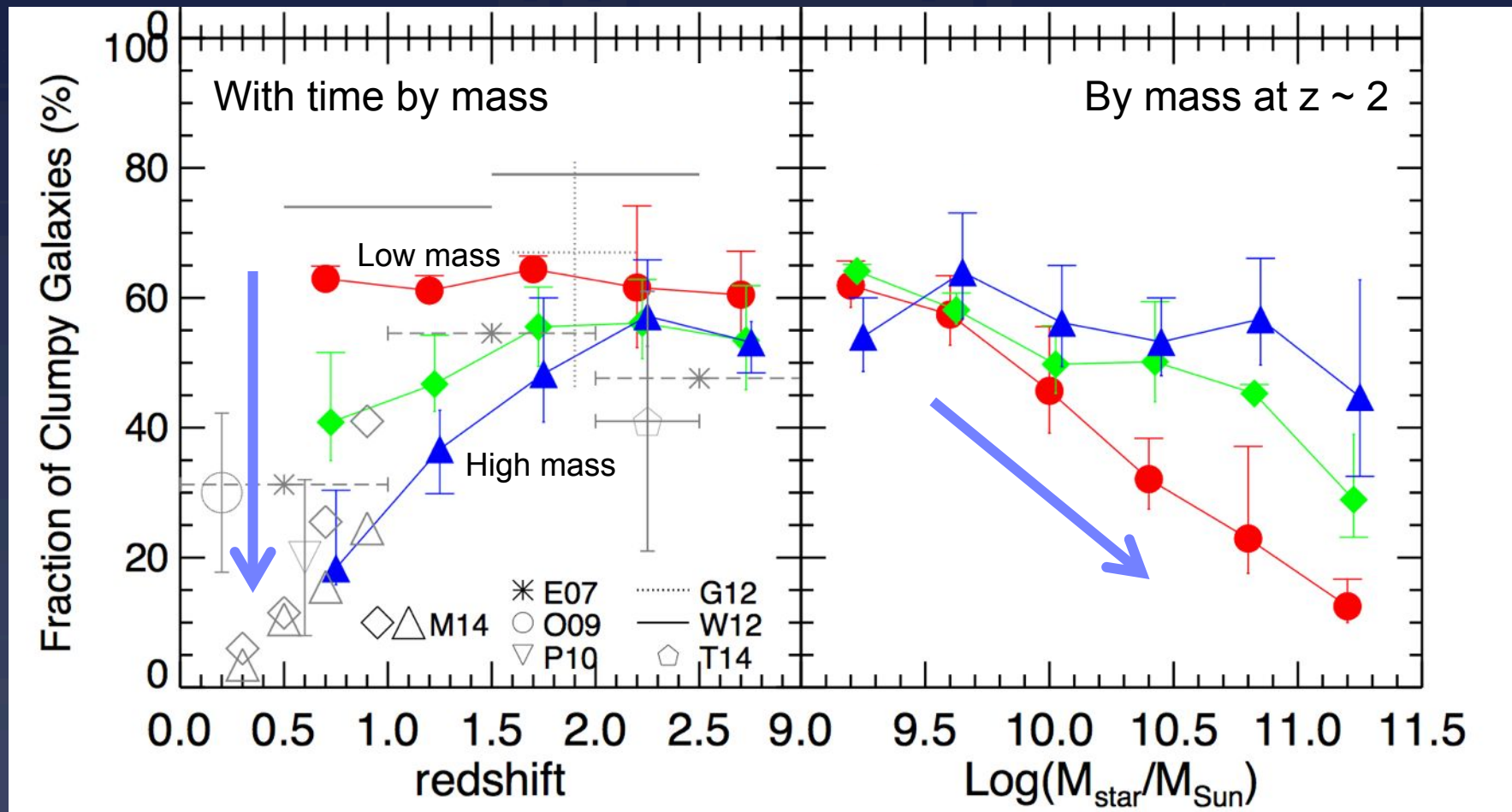
FIG. 7.— Identical to Figure 5, but with the color-coding indicating the normalized stellar surface mass density. When considering shorter wavelengths (i.e., poorer proxies of stellar mass), little variation in the stellar surface mass density is seen at a given radius, despite a substantial range in surface brightness levels.

Clumps in massive galaxies at $1 < z < 2$ account for $\sim 20\%$ of the star formation but 7% of the mass. Centers are older.

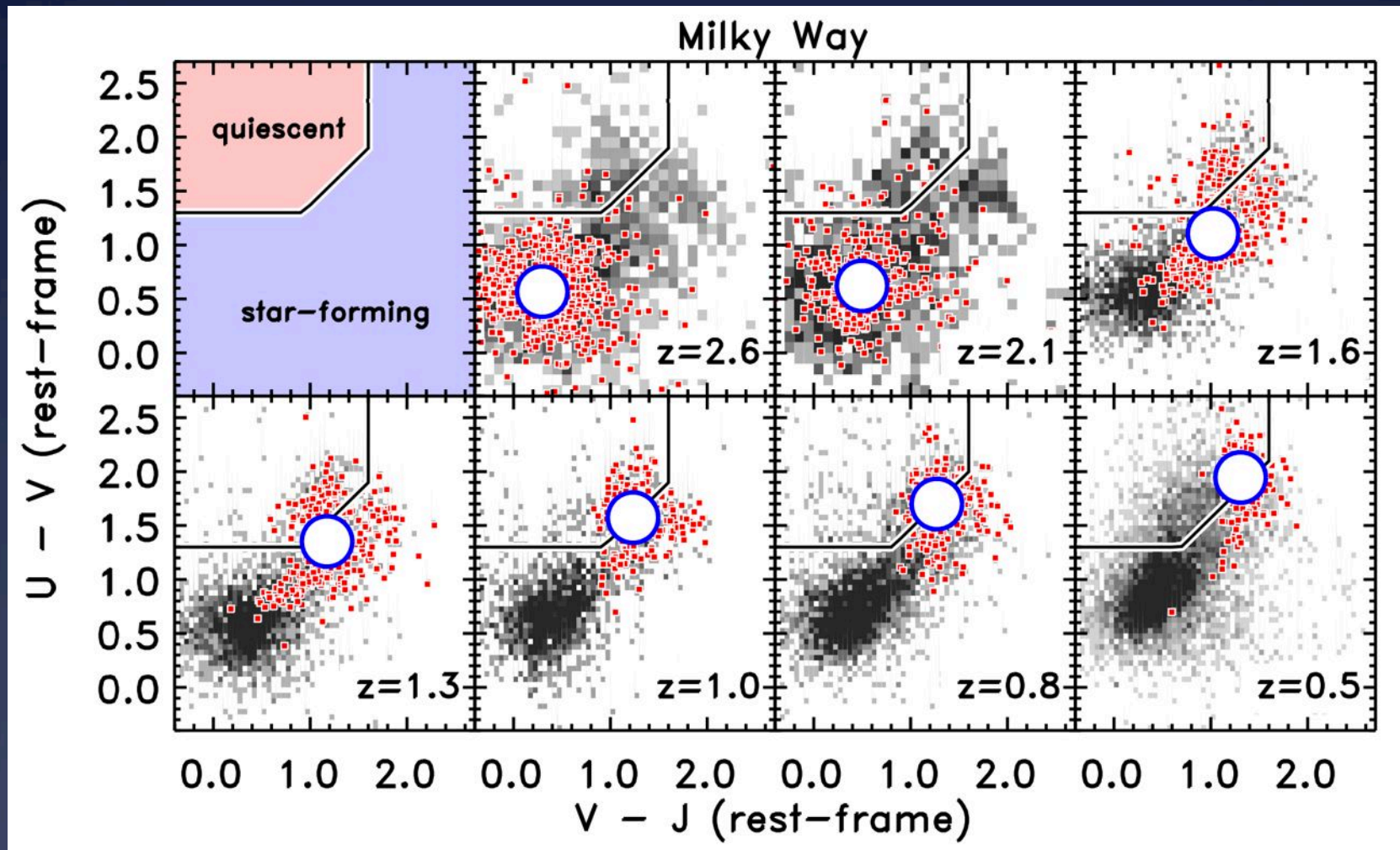
Wuyts+13

Clump fraction falls with both mass and with time “Morphological downsizing” again

Prolate structures have implications for instability modeling

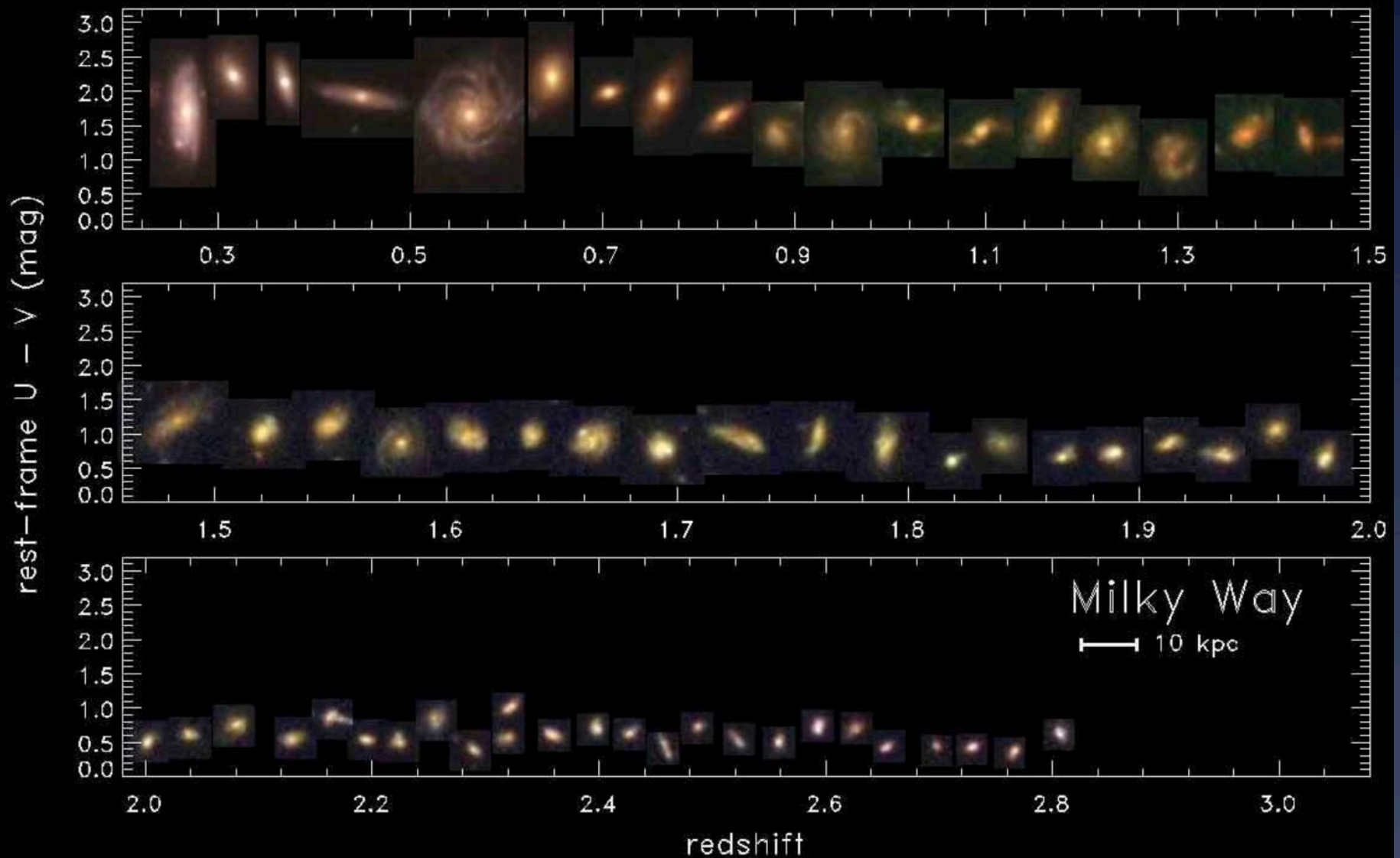


What did the Milky Way look like 11 billion years ago?



Papovich+14 in prep (CANDELS + ZFOURGE)

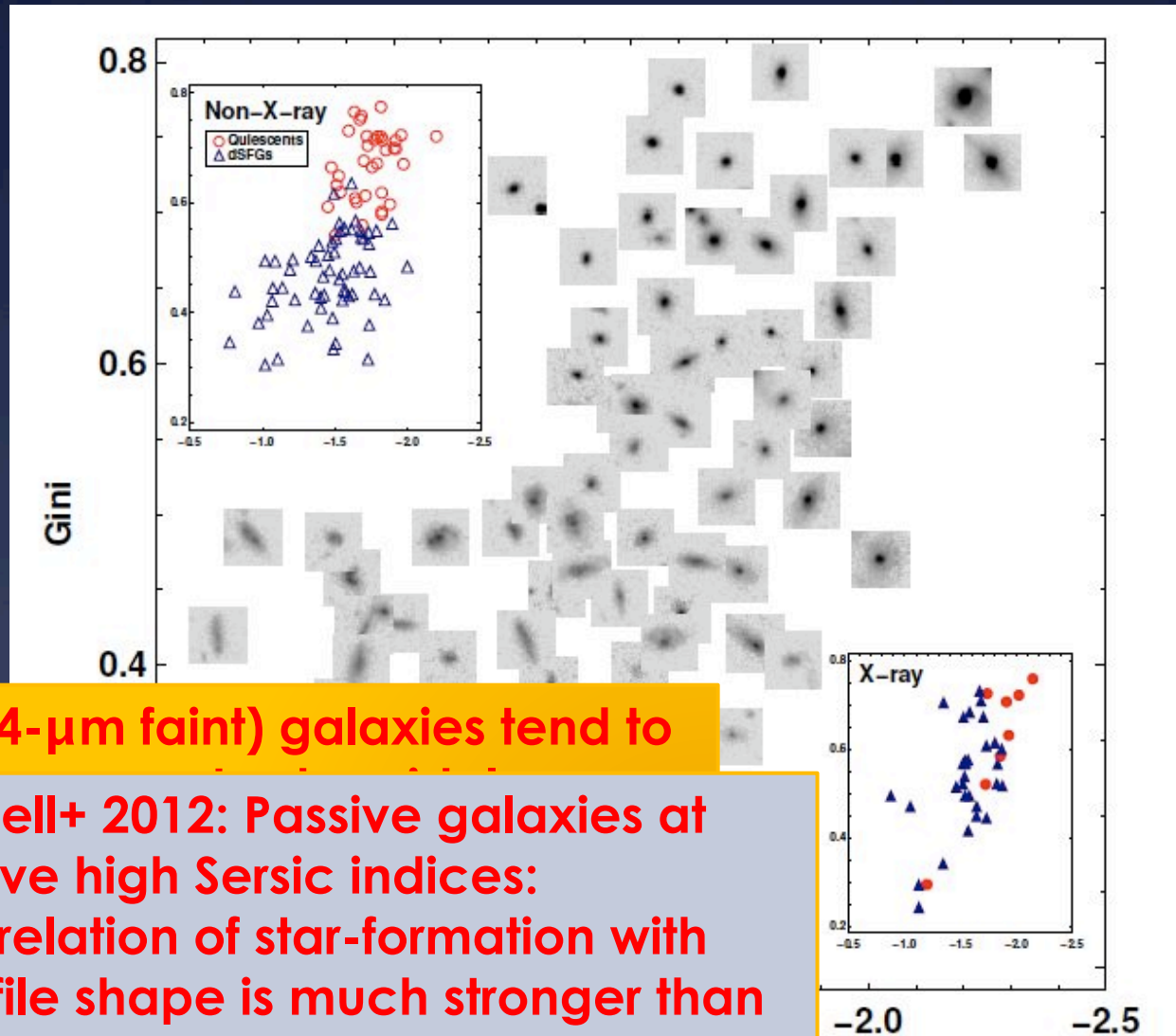
What did the Milky Way look like 11 billion years ago?



Star-formation rate, morphology and size
are strongly linked above $z \sim 2$

Quenching \leftrightarrow spheroid \leftrightarrow dense

The best predictor of a galaxy's specific star-formation rate at $z \sim 2$ is its morphology.



Passive (24- μm faint) galaxies tend to

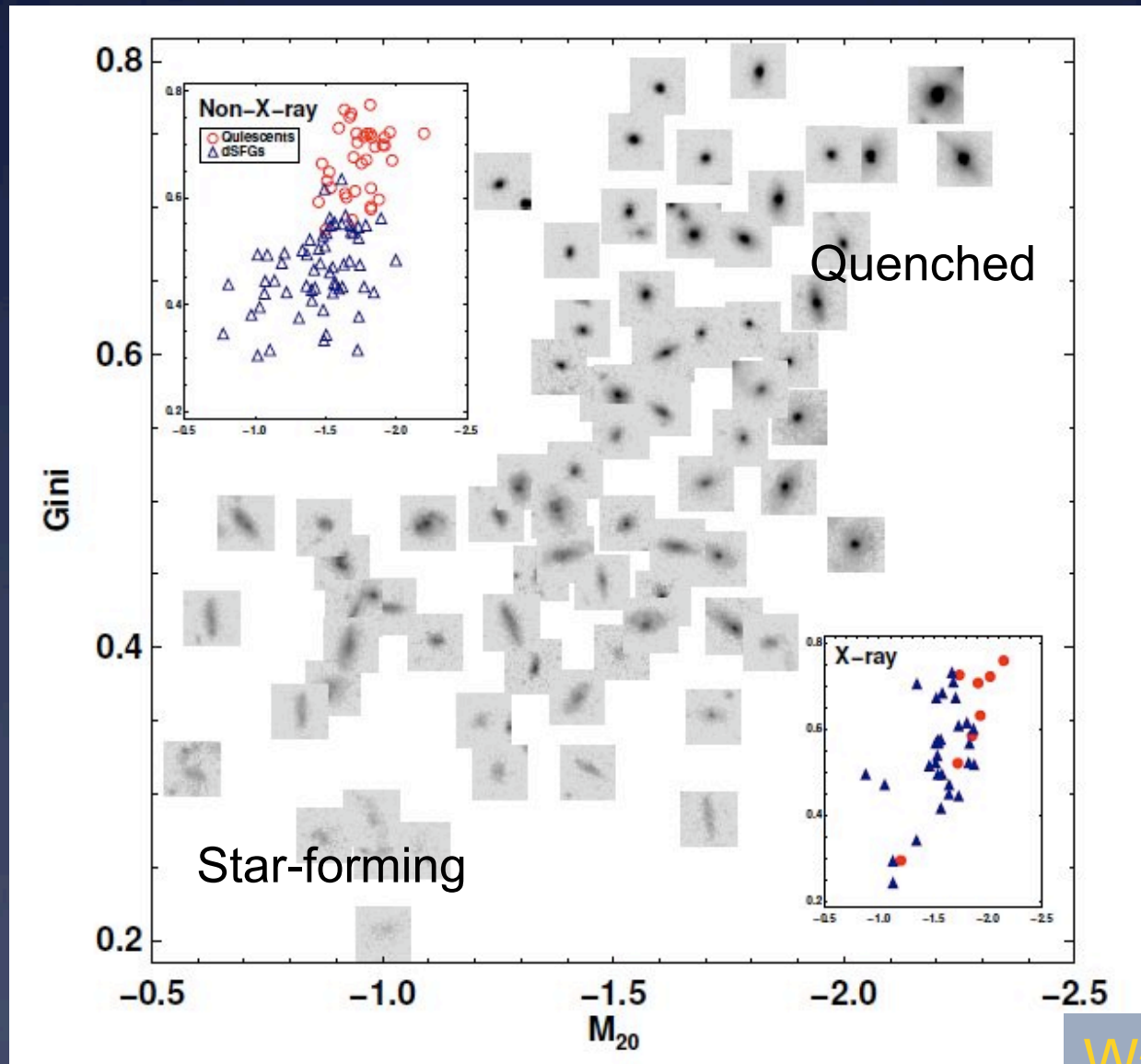
Star

Also, Bell+ 2012: Passive galaxies at $z \sim 2$ have high Sersic indices:

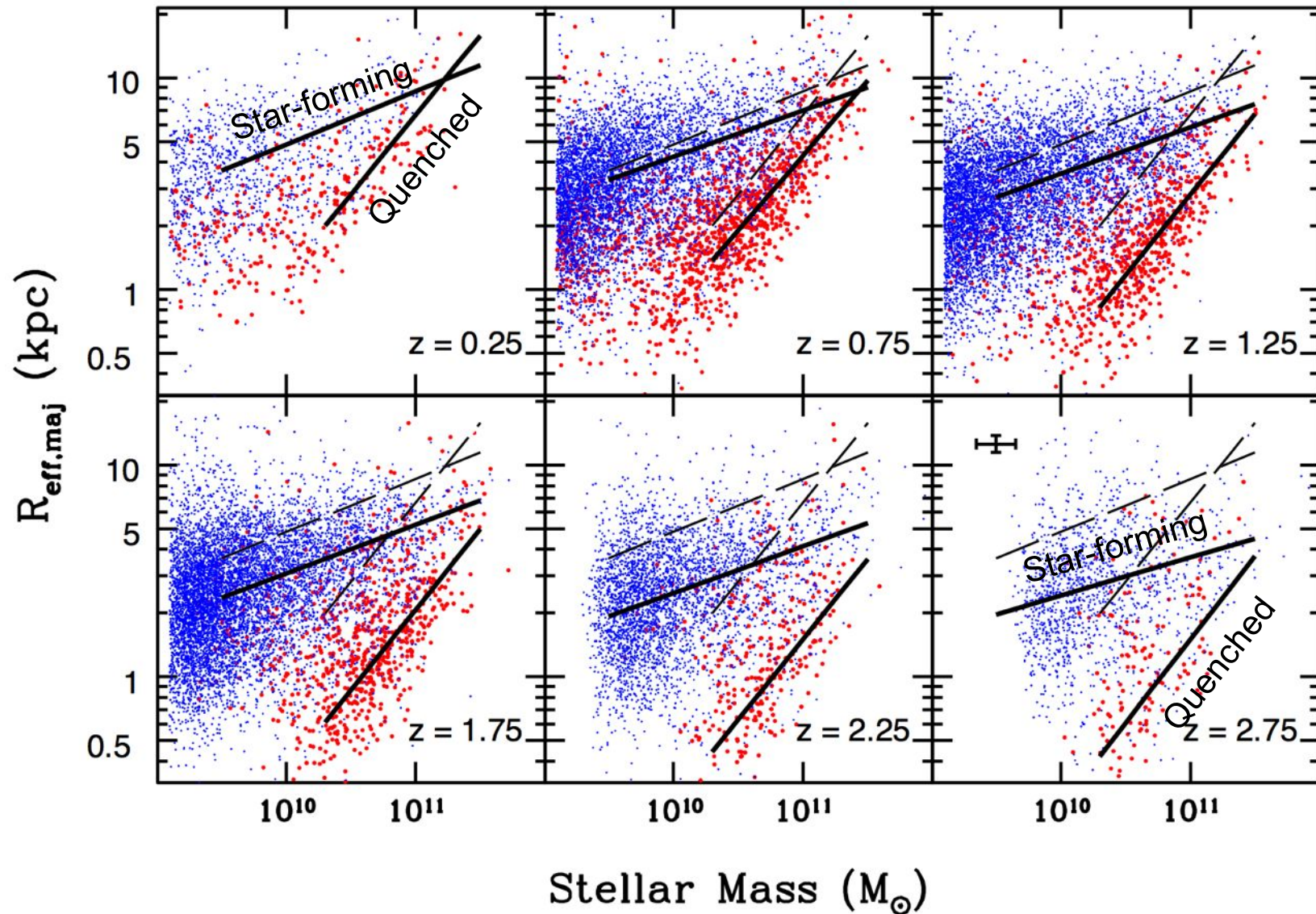
- Correlation of star-formation with profile shape is much stronger than with stellar mass.

Wang+ 2012

The best predictor of a galaxy's specific star-formation rate at $z \sim 2$ is its morphology.



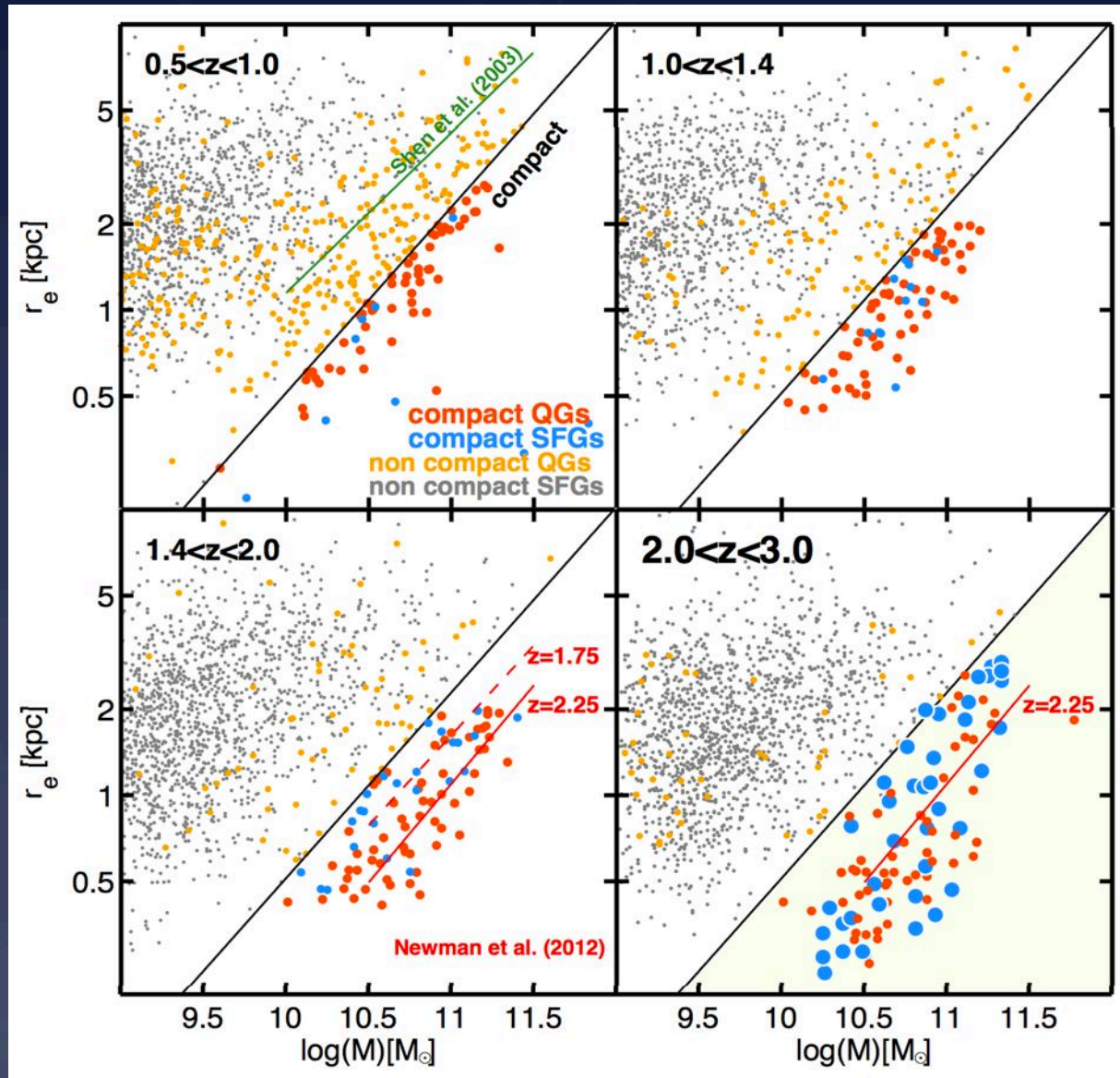
SFR vs. quenched galaxies obey separate mass-radii relations



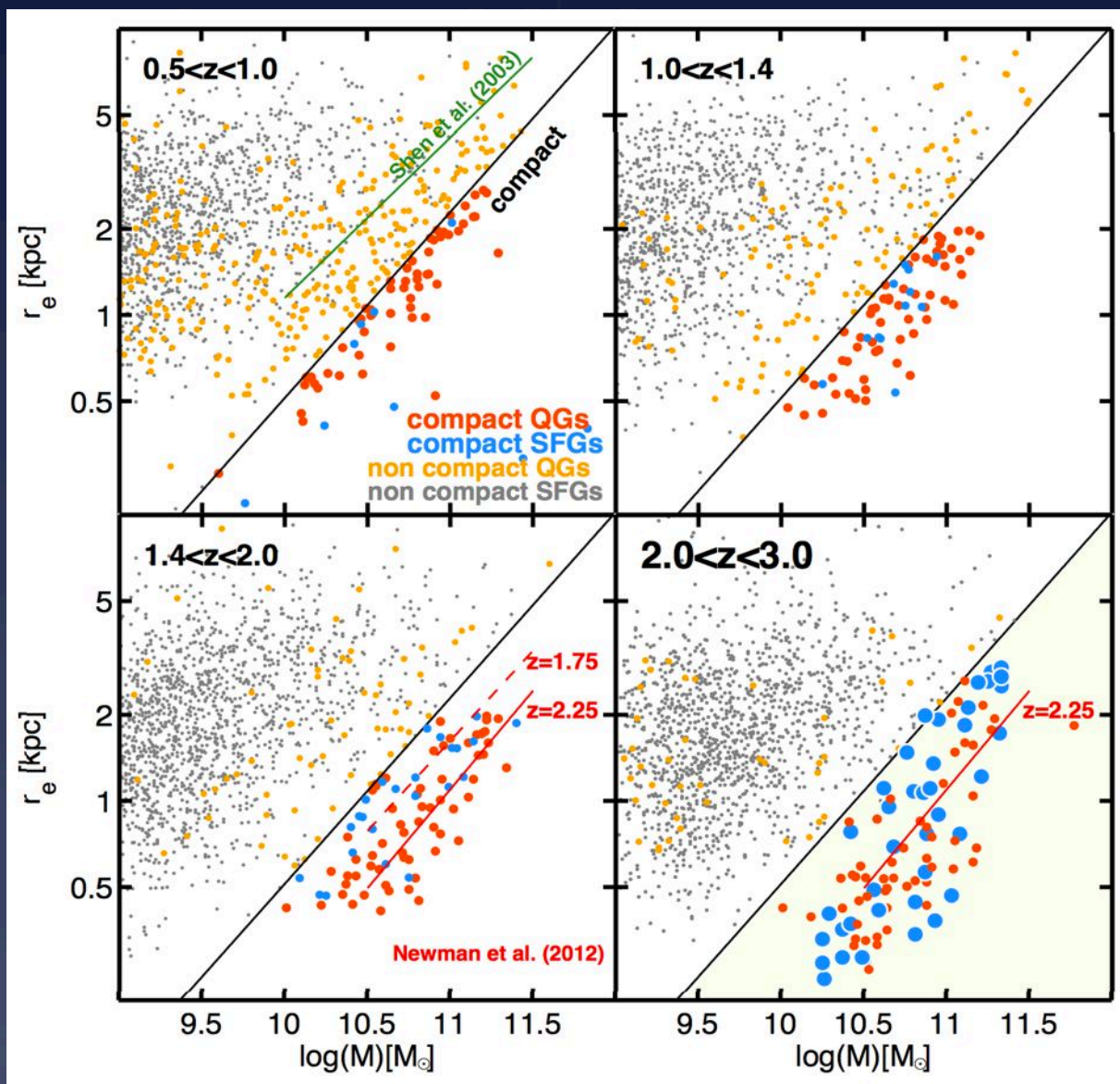
Massive, quenched galaxies at $z \sim 2$ are
physically small

Morphological transformation precedes
quenching

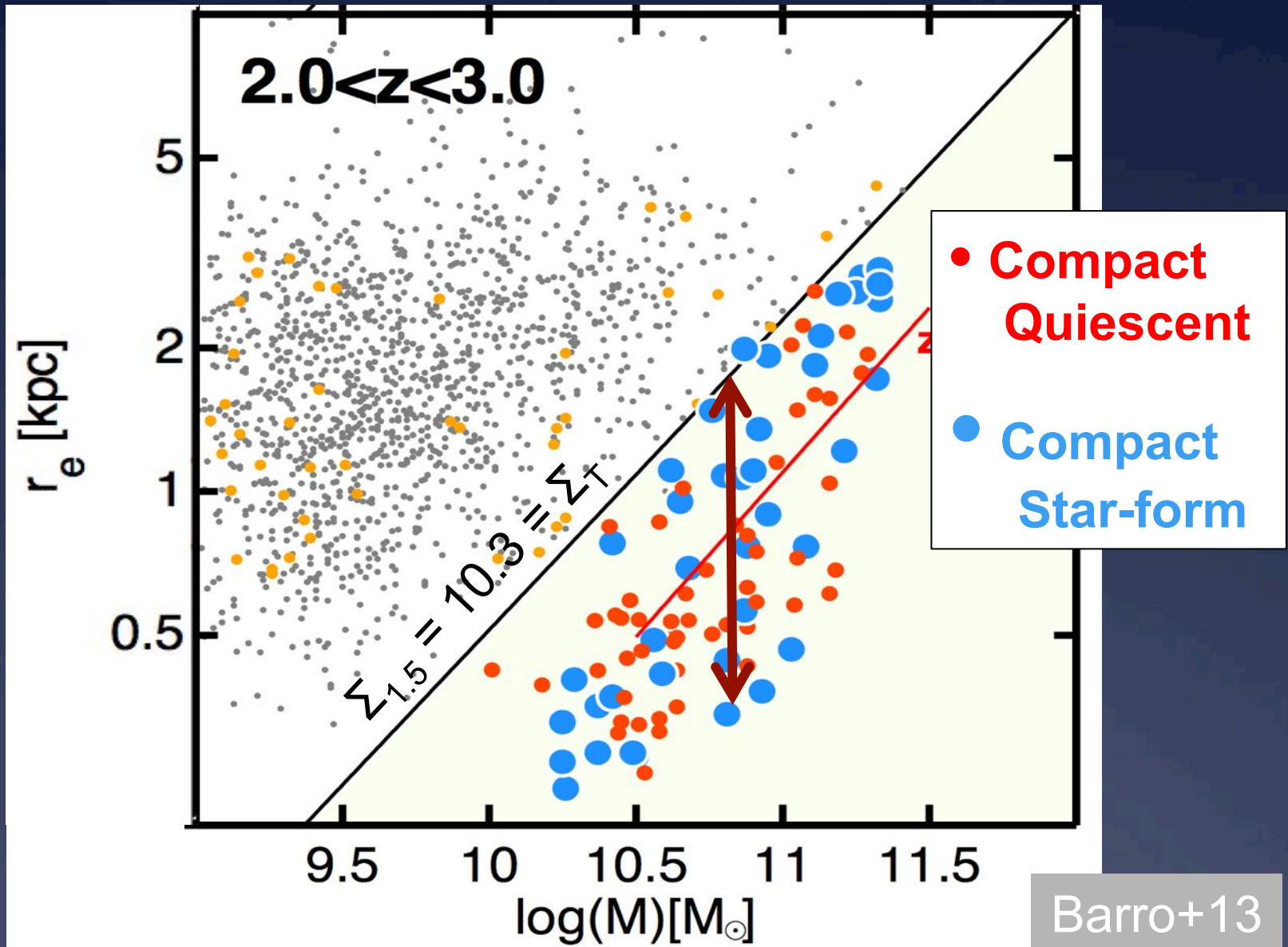
Massive, quenched galaxies at $z \sim 2$ are physically small



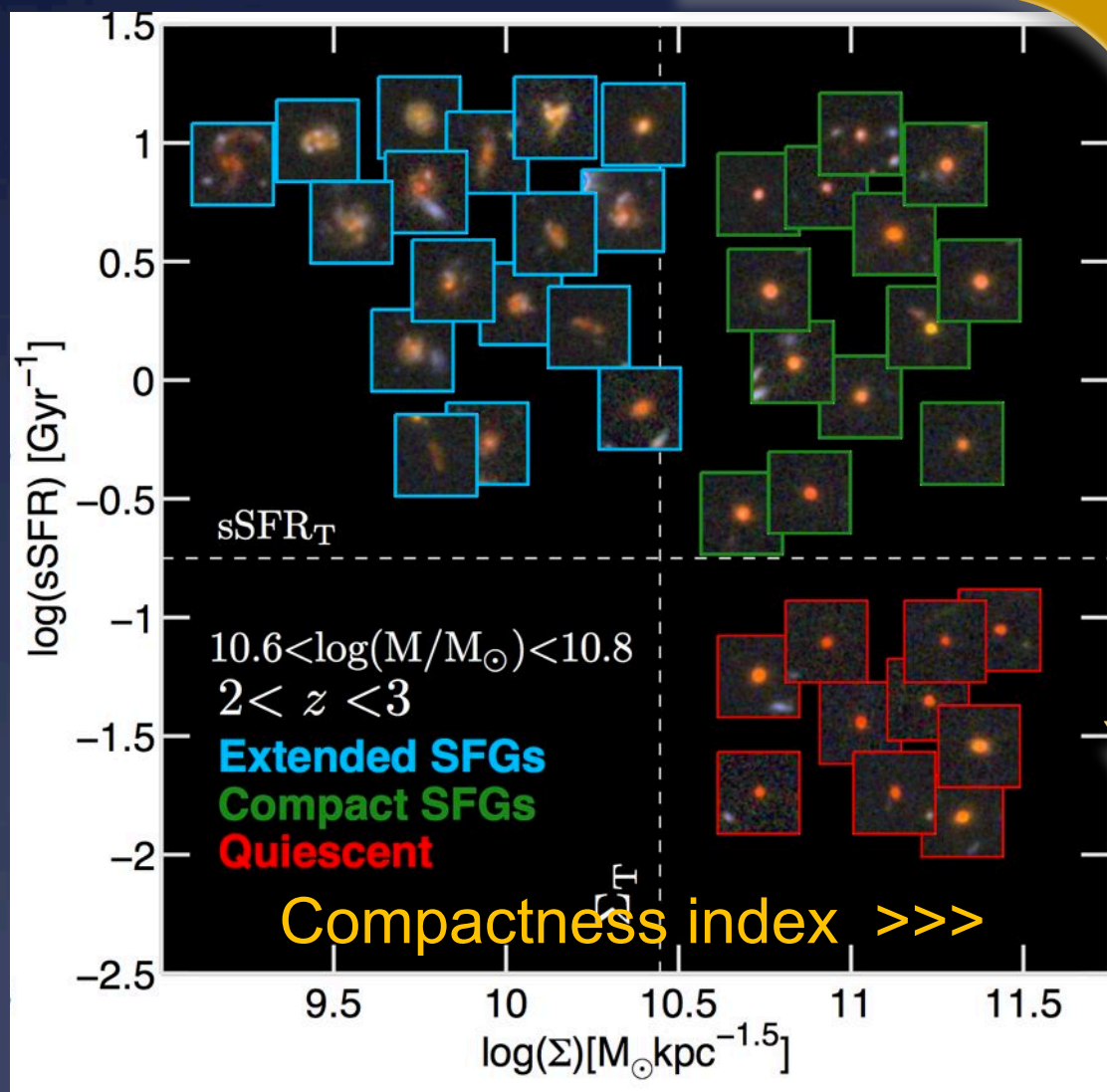
Star-forming galaxies co-exist with same mass and size



Define a “compactness” index, $\Sigma_{1.5}$



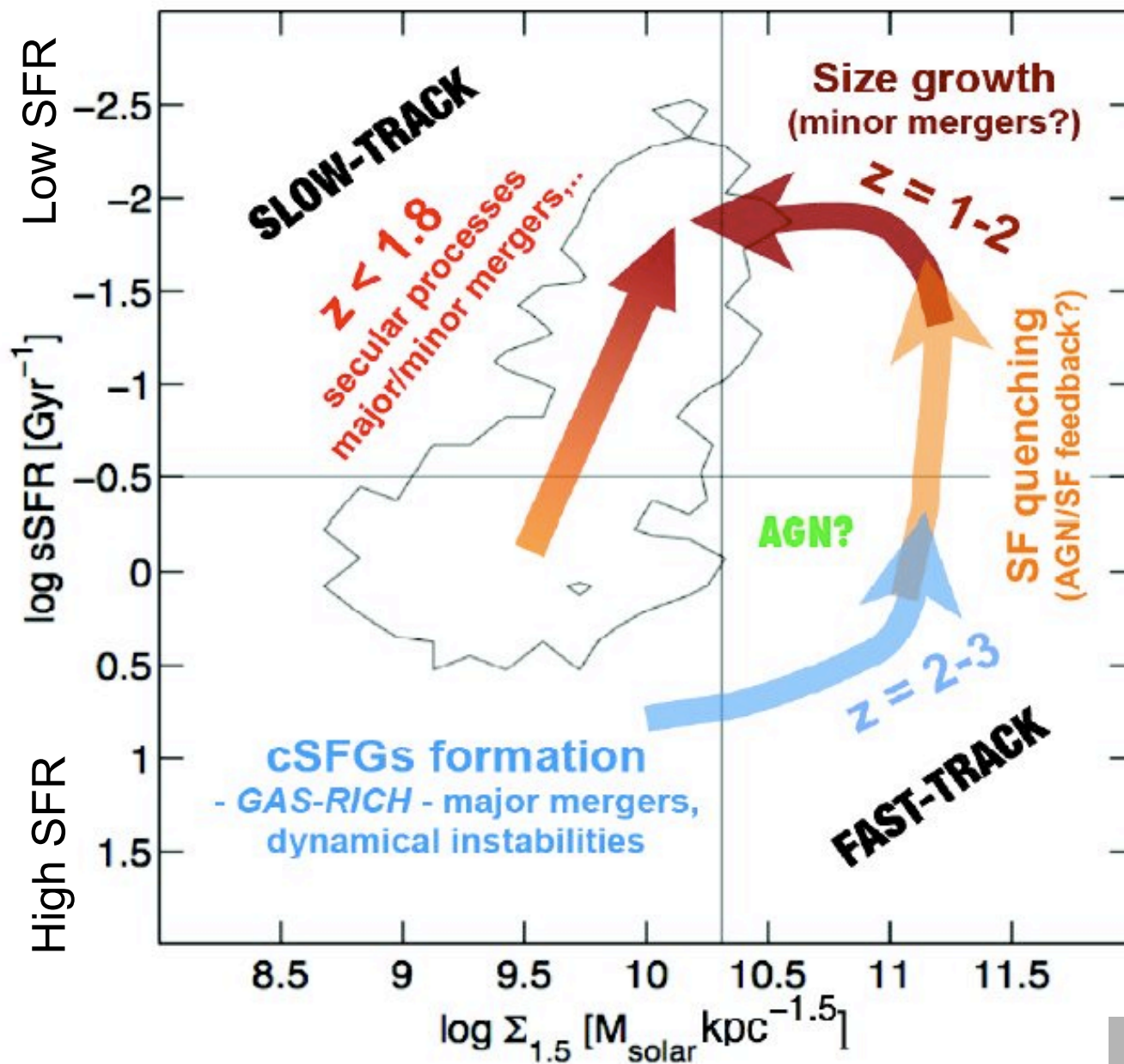
Morphological transformation precedes quenching



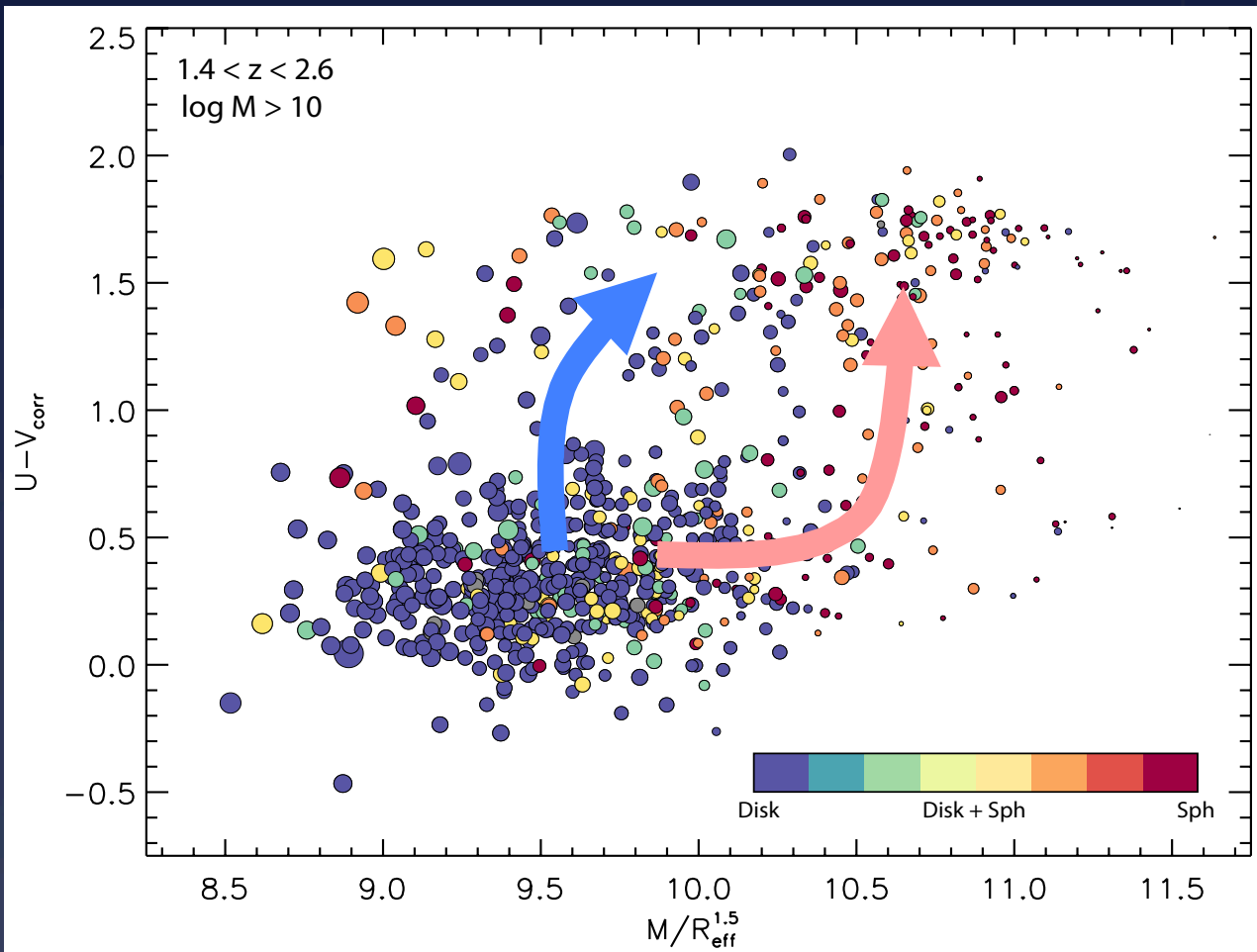
Galaxies become compact before quenching

Direction of evolution

Barro+ 14
Williams+ 14

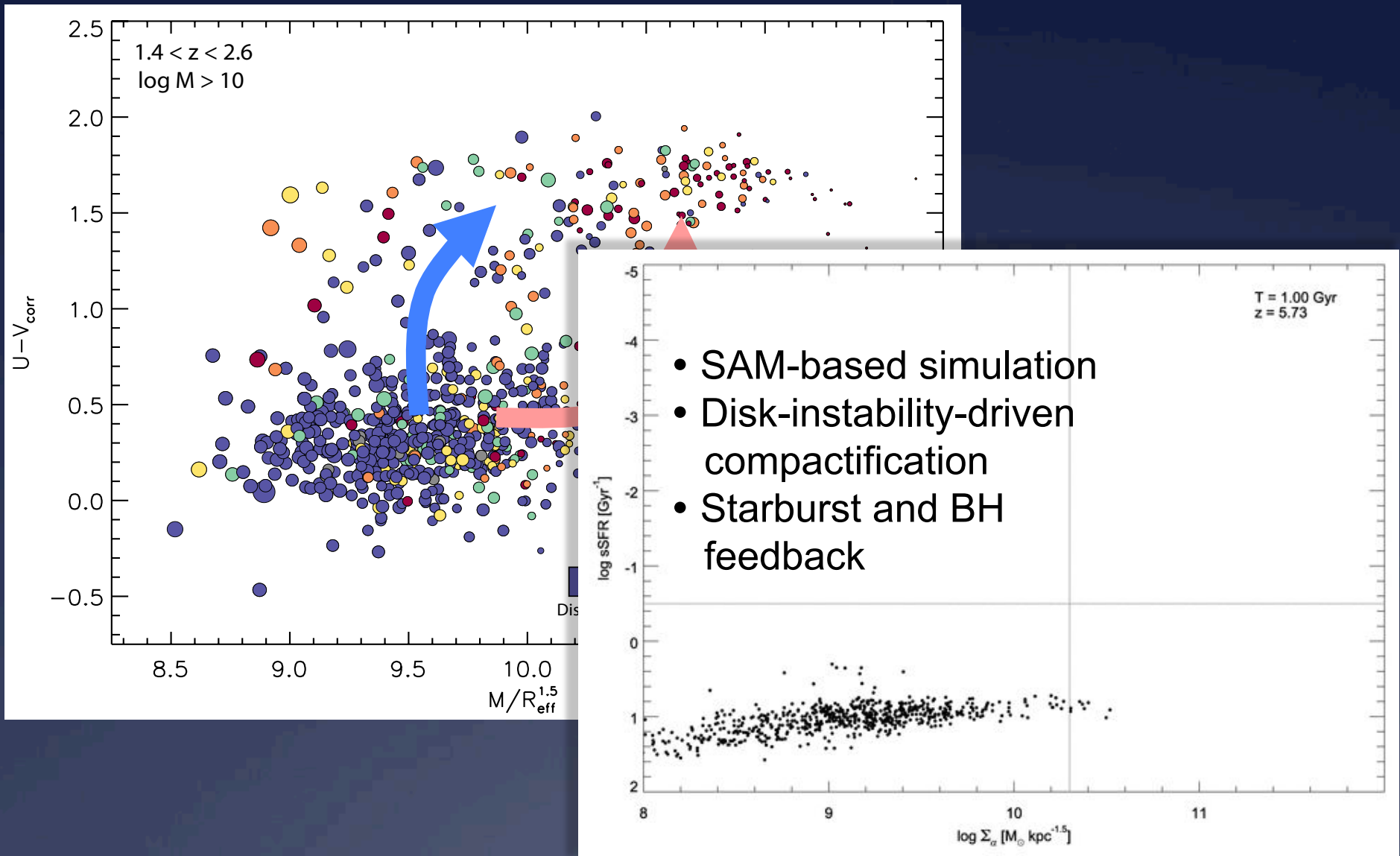


Fast quenching at $z \sim 2$ due to violent-disk-instability AGNs



Courtesy Lauren Porter, Rachel Somerville & Joel Primack

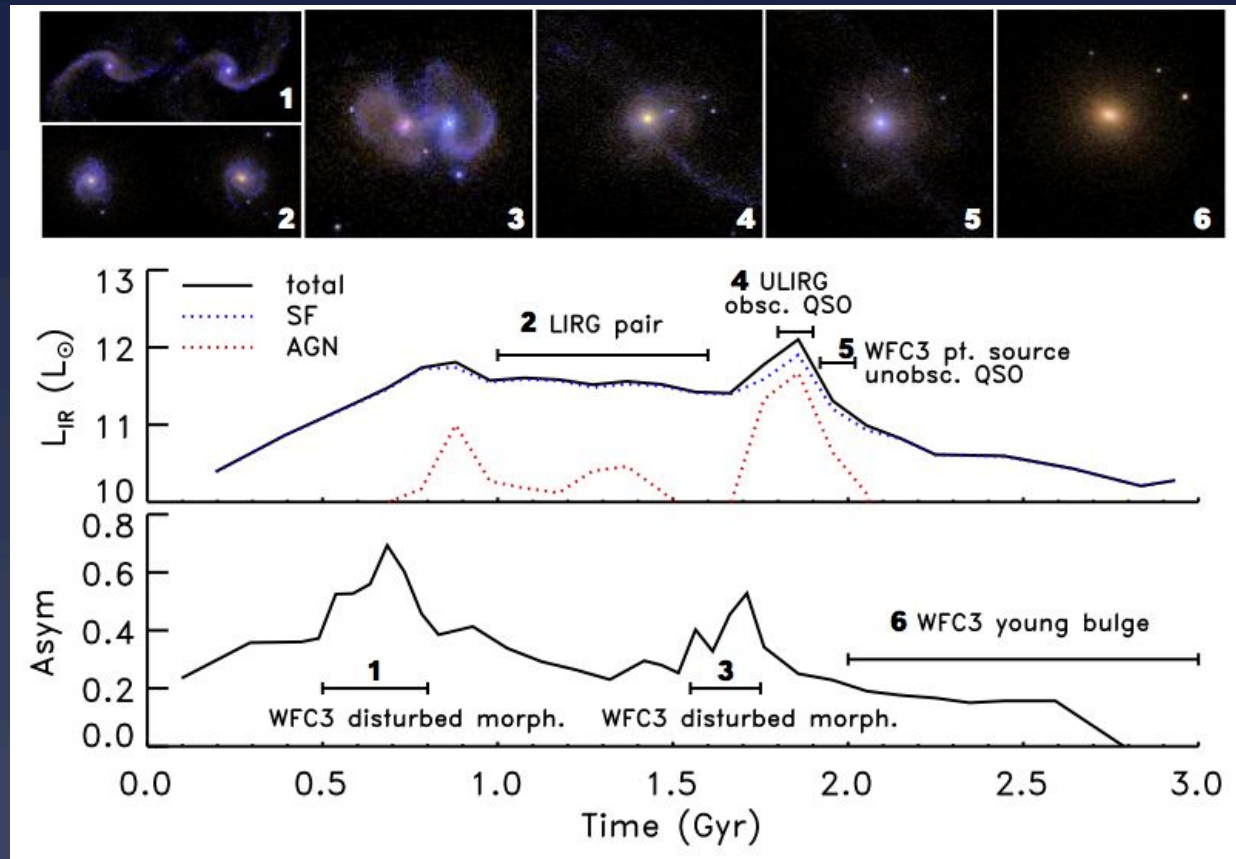
Fast quenching at $z \sim 2$ due to violent-disk-instability AGNs



Courtesy Lauren Porter, Rachel Somerville & Joel Primack

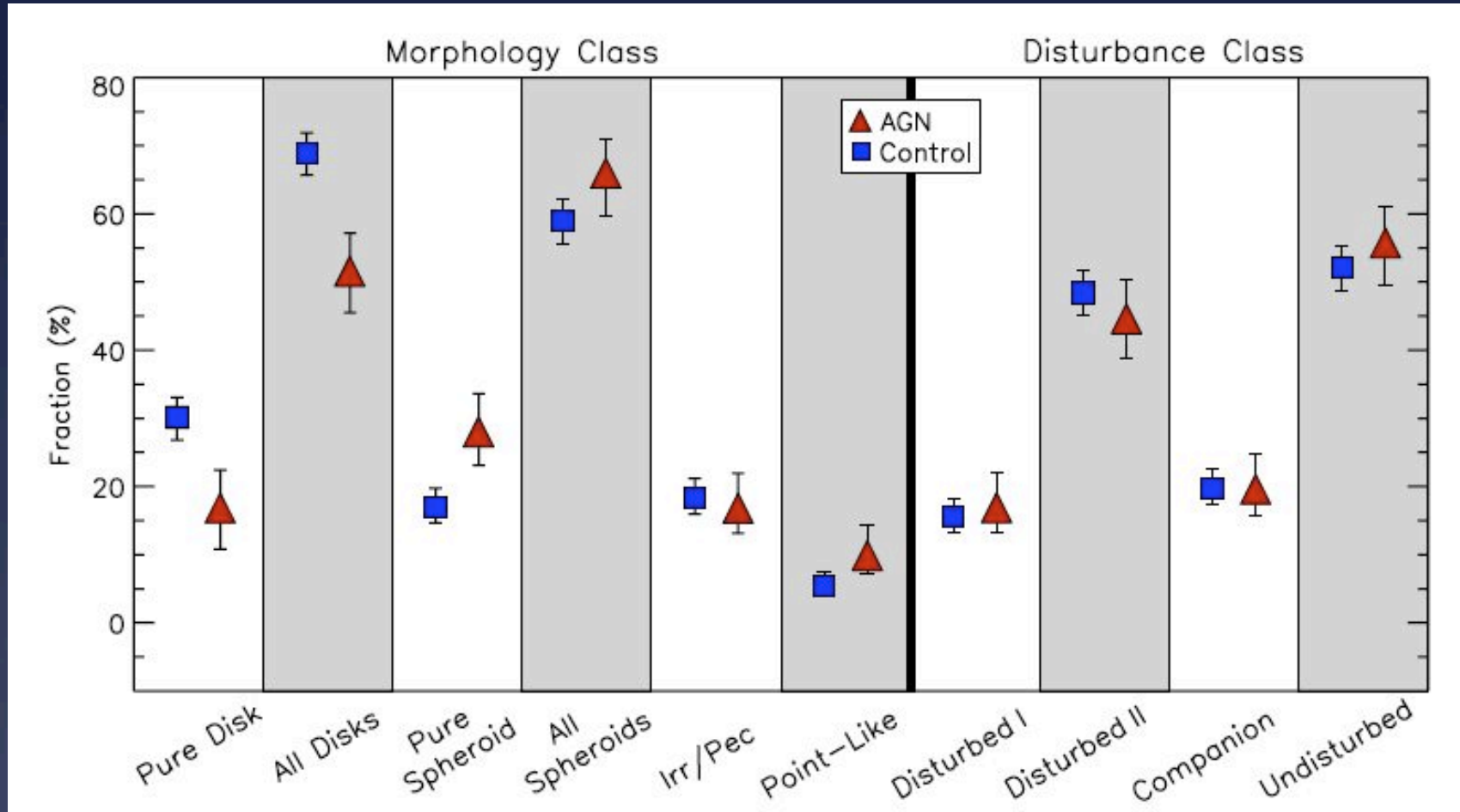
4 Cosmic Noon AGNs

Pre-CANDELS prediction for fueling $z \sim 2$ AGN

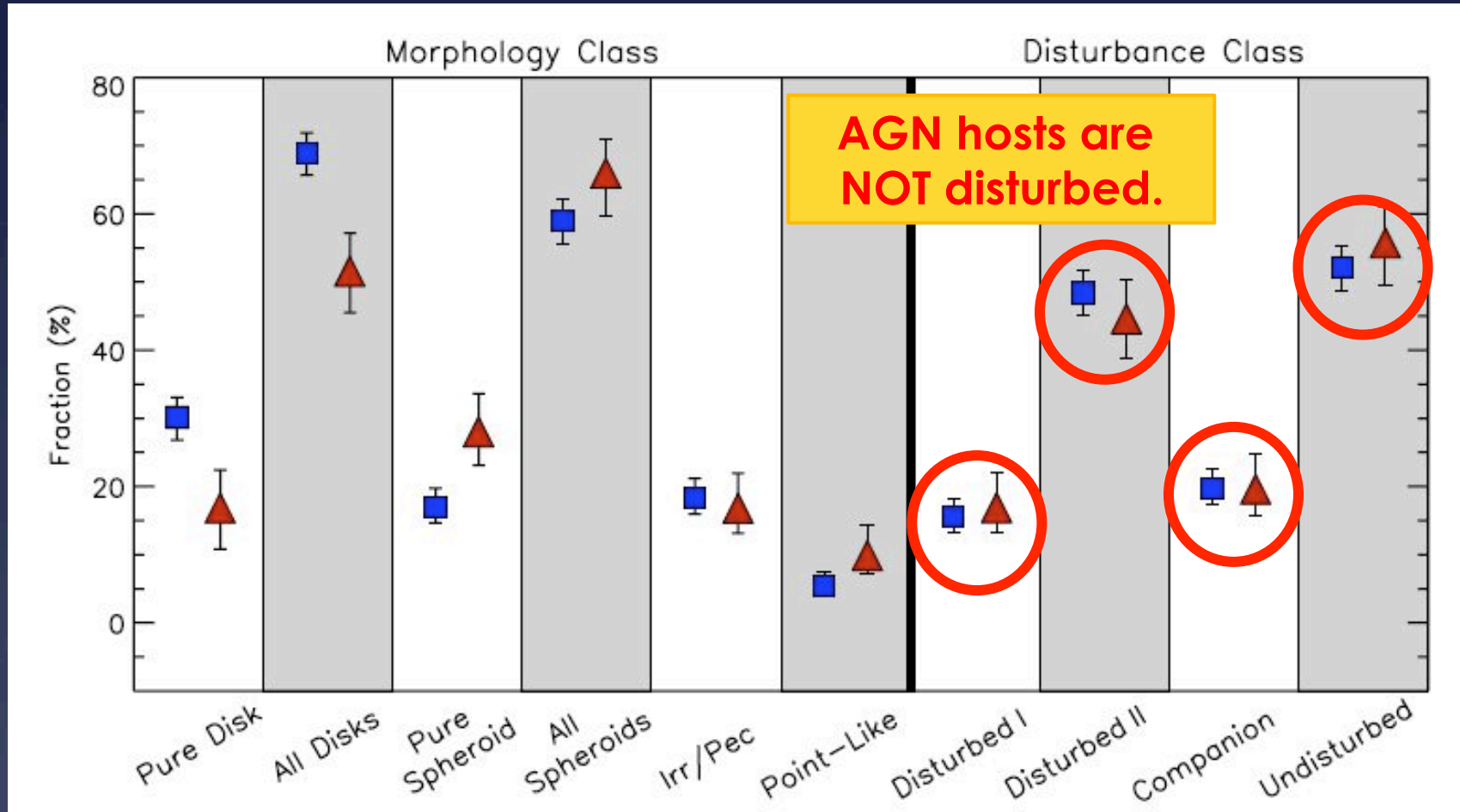


Popular scenario: Merger \rightarrow ULIRG \rightarrow
embedded QSO \rightarrow unobscured AGN \rightarrow
elliptical galaxy with black hole (e.g., Hopkins+ 06)

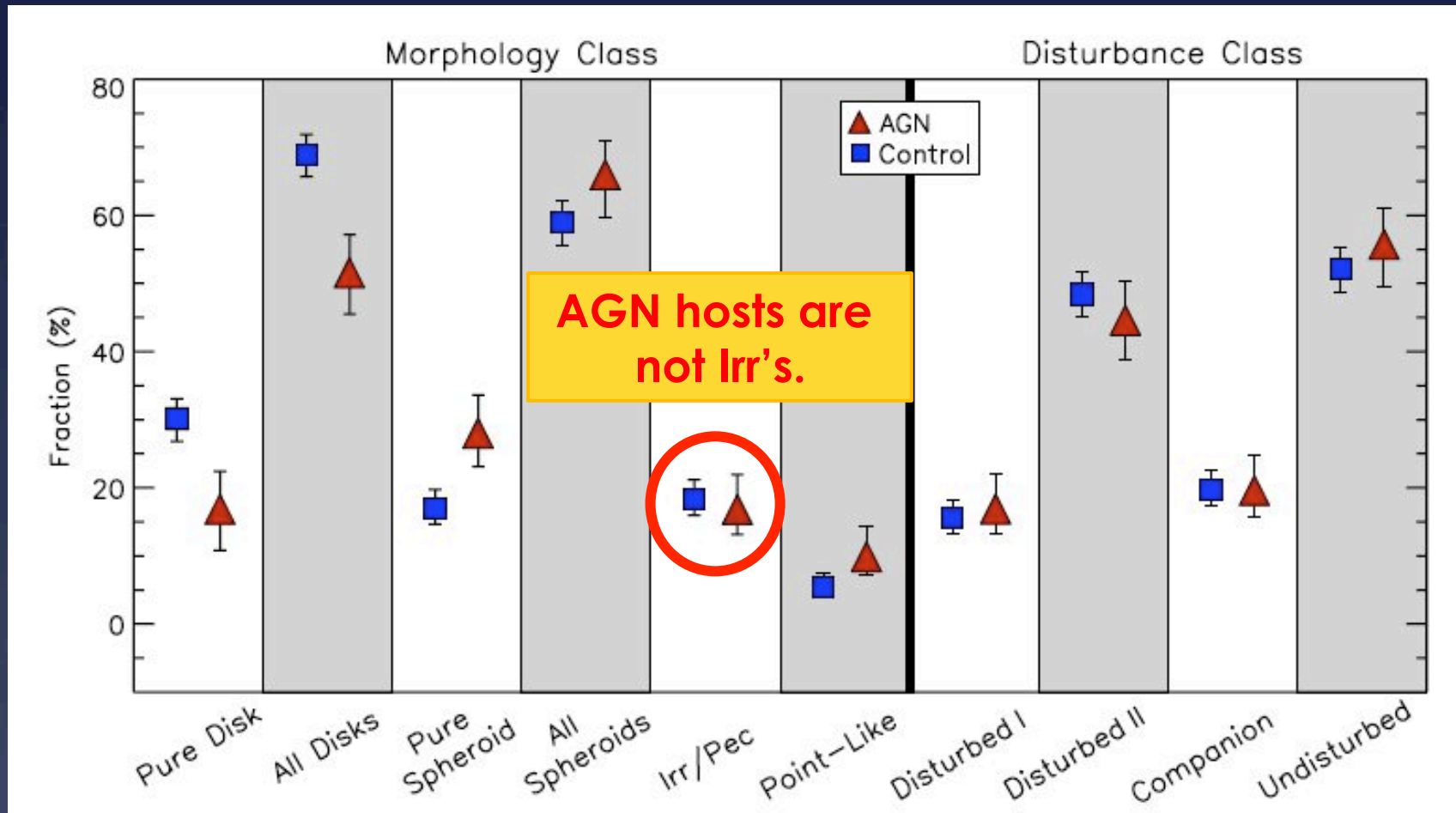
Mergers do not play a significant role in fueling the central supermassive black holes in most x-ray selected active galaxies at $z \sim 2$.



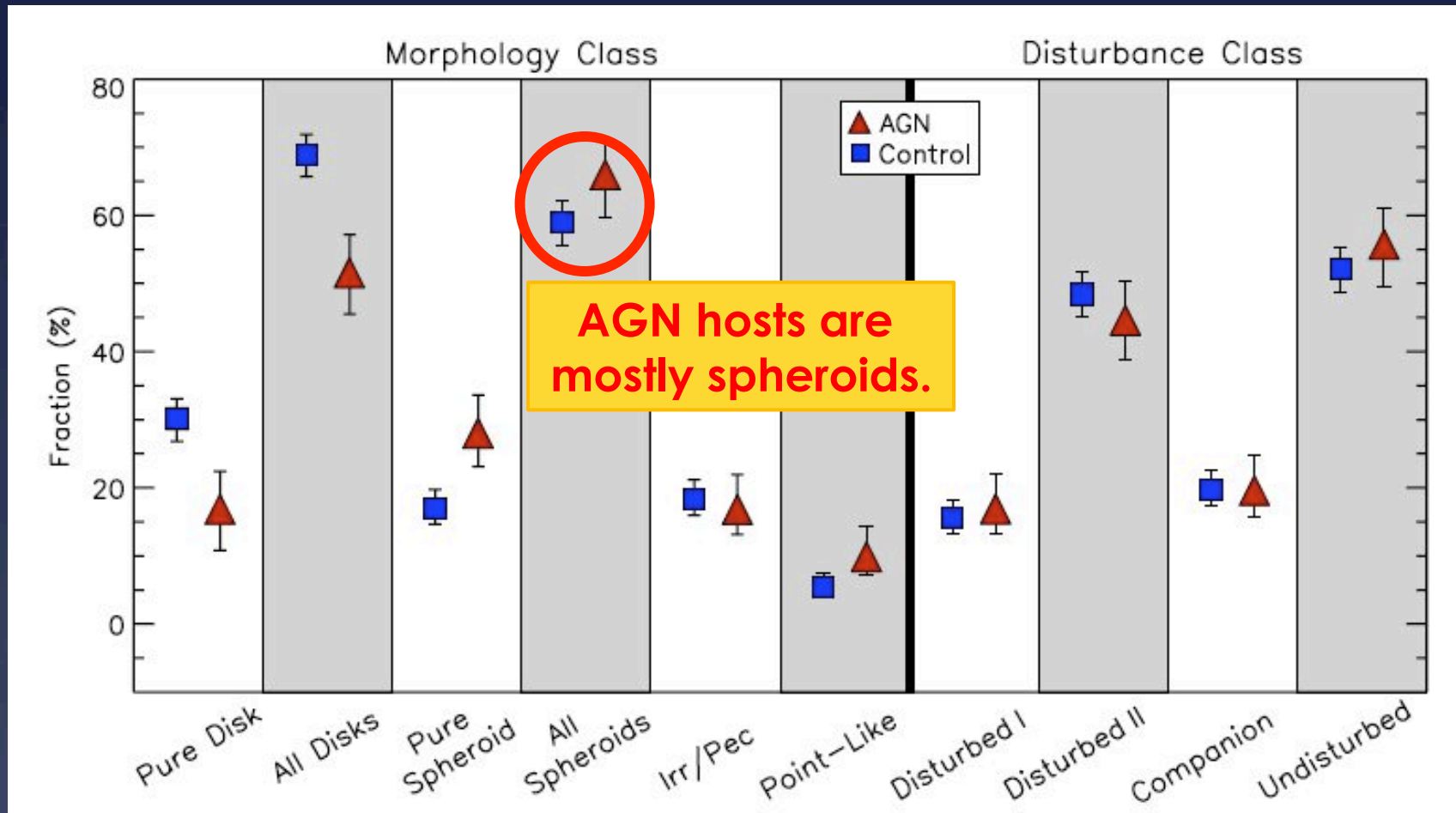
Mergers do not play a significant role in fueling the central supermassive black holes in most x-ray selected active galaxies at $z \sim 2$.



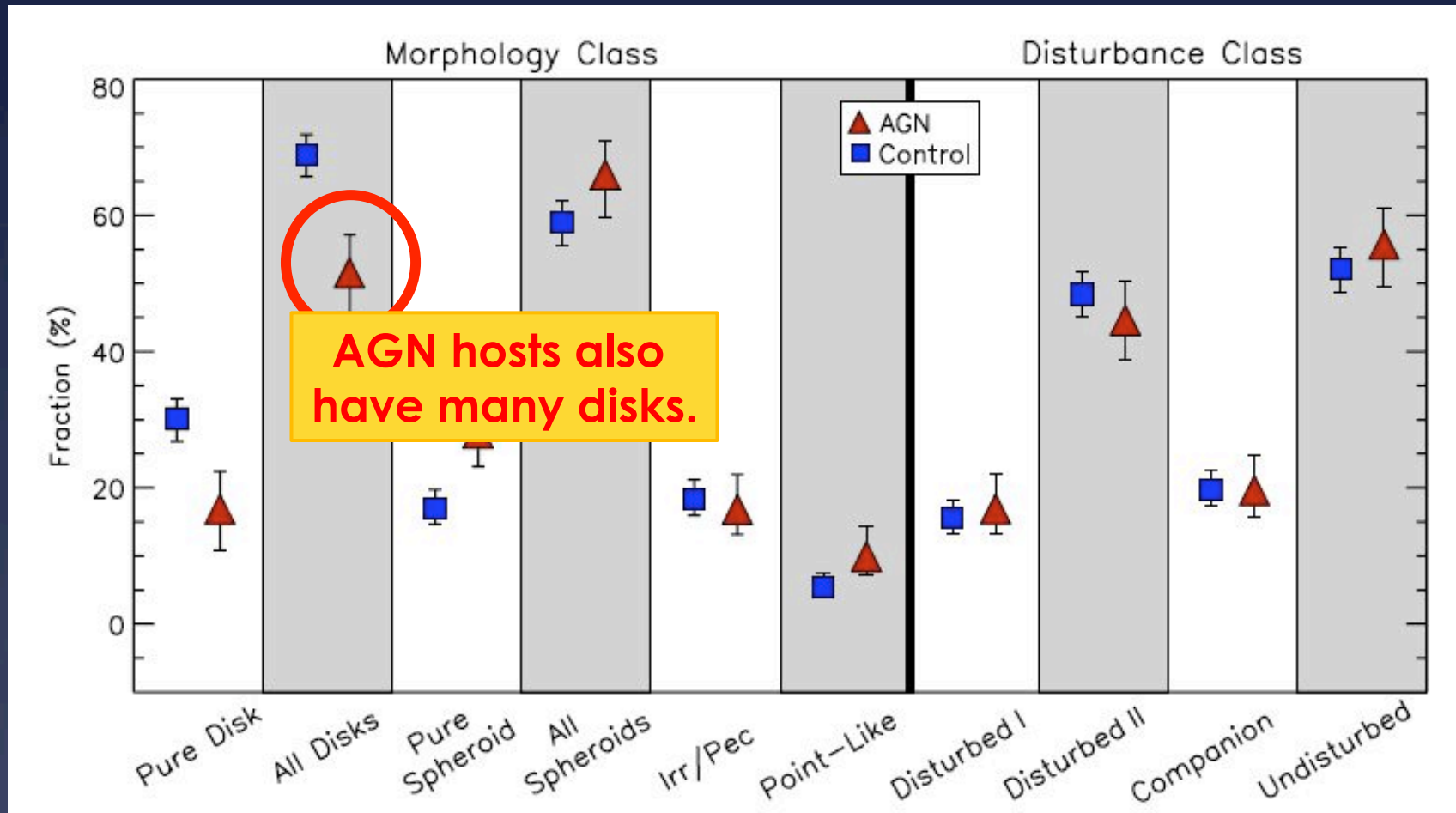
Mergers do not play a significant role in fueling the central supermassive black holes in most x-ray selected active galaxies at $z \sim 2$.



Mergers do not play a significant role in fueling the central supermassive black holes in most x-ray selected active galaxies at $z \sim 2$.



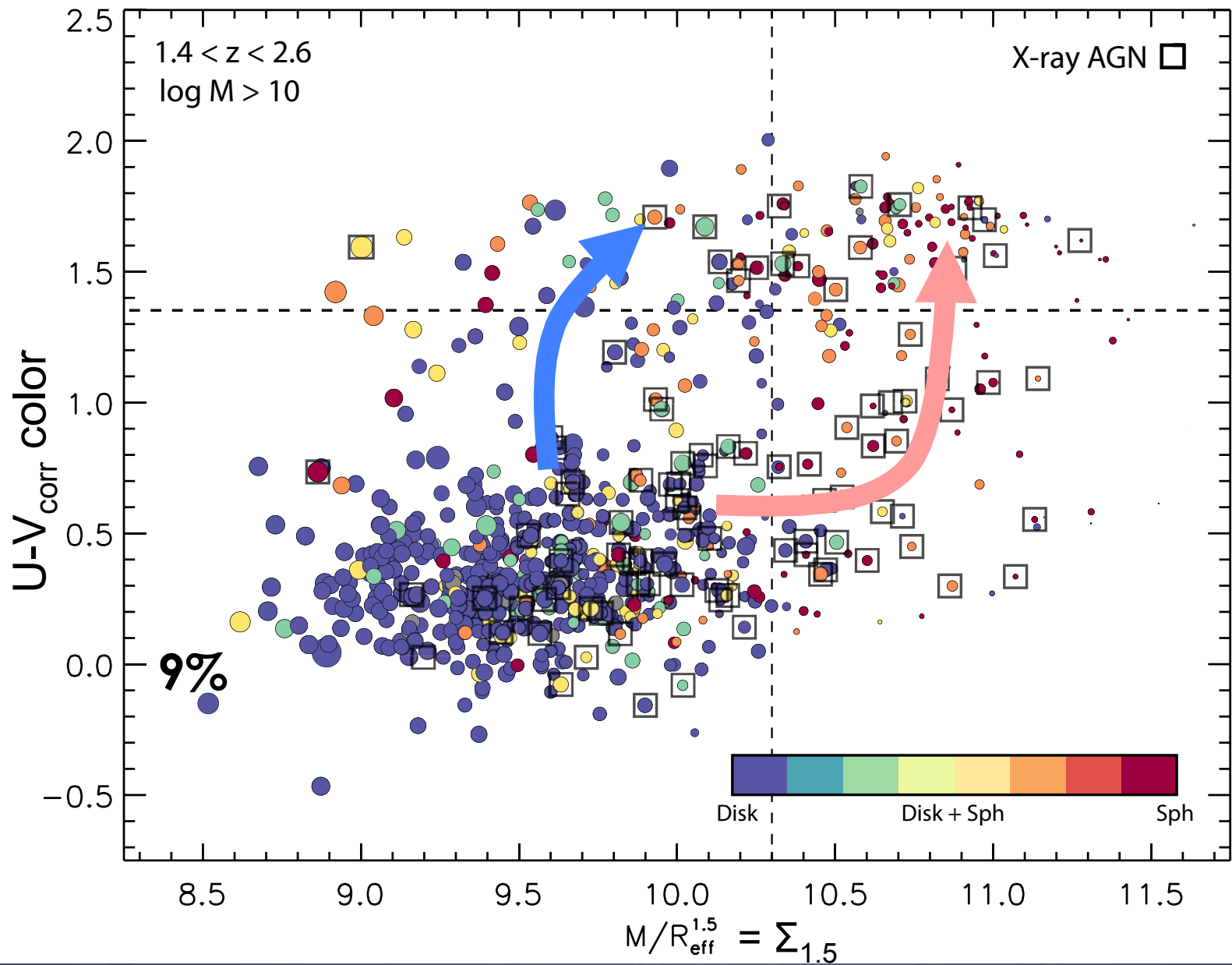
Mergers do not play a significant role in fueling the central supermassive black holes in most x-ray selected active galaxies at $z \sim 2$.



Mergers do not play a significant role in fueling the central supermassive black holes in most x-ray selected active galaxies at $z \sim 2$.

- Possible explanations:
 - Mergers are important only for the most luminous AGN
 - AGN at lower luminosities are internally triggered, e.g. by disk instabilities.
 - Disks are more persistent in gas-rich mergers than thought; disks can rebuild
 - X-ray AGN are a late phase; AGN are still dust obscured when the merger signatures are most apparent
 - AGN variability (Hickox+ 14)

AGN at the quenching threshold



AGN at the quenching threshold

